A Generic and Intelligent Approach of Feed Rate Determination for CNC Profile Milling

Zhibin Miao

A Thesis

in

the Department

of

Mechanical & Industrial Engineering

Presented in Partial Fulfillment of the Requirements

for the Degree of Master of Applied Science (Mechanical Engineering) at

Concordia University

Montreal, Quebec, Canada

August 2004

© ZHIBIN MIAO, 2004

Library and Archives Canada

Published Heritage Branch

395 Wellington Street
Ottawa ON K1A 0N4
Canada

Bibliothèque et Archives Canada

Direction du Patrimoine de l'édition

395, rue Wellington
Ottawa ON K1A 0N4
Canada

Your file Votre référence
ISBN: 0-612-94731-9
Our file Notre référence
ISBN: 0-612-94731-9

The author has granted a non-exclusive license allowing the Library and Archives Canada to reproduce, loan, distribute or sell copies of this thesis in microform, paper or electronic formats.

L'auteur a accordé une licence non exclusive permettant à la Bibliothèque et Archives Canada de reproduire, prêter, distribuer ou vendre des copies de cette thèse sous la forme de microfiche/film, de reproduction sur papier ou sur format électronique.

The author retains ownership of the copyright in this thesis. Neither the thesis nor substantial extracts from it may be printed or otherwise reproduced without the author's permission.

L'auteur conserve la propriété du droit d'auteur qui protège cette thèse. Ni la thèse ni des extraits substantiels de celle-ci ne doivent être imprimés ou aturement reproduits sans son autorisation.

In compliance with the Canadian Privacy Act some supporting forms may have been removed from this thesis.

Conformément à la loi canadienne sur la protection de la vie privée, quelques formulaires secondaires ont été enlevés de cette thèse.

While these forms may be included in the document page count, their removal does not represent any loss of content from the thesis.

Bien que ces formulaires aient inclus dans la pagination, il n'y aura aucun contenu manquant.

Canada

Abstract

A Generic and Intelligent Approach of Feed Rate Determination for CNC Profile Milling

Zhibin Miao

Determination of optimal machining parameters - spindle rate, feed rate, and depth of cut - has been a research topic for decades. Since the parameters of CNC machining significantly influence part machining time, part surface quality, and tool life, techniques of determining optimal machining parameters are in high demand in manufacturing industry. Usually the depth of cut and spindle rate are determined according to machinist manuals before machining; and the feed rate is determined subjectively either by CNC machine operators or programmers. As a result, the feed rate is not optimal in terms of the machining condition at every cutter location, and it is fixed at a conservative value causing longer machining time or shorter tool life. In this work, a generic and intelligent approach of feed rate determination for CNC profile milling is proposed. First a two-dimension chip load model is introduced and an example database of machining parameters is presented. Second a fuzzy rule-based system is established to predict the cutting force based on the radial and axial depths of cut, and the assumed feed rate. The next step is to identify the geometric features of the part, calculate the engagement angles of the geometric features, and find proper feed rates for them. Finally the approach is applied on an example part for profile milling, and the results are simulated with CATIA CAD/CAM system to demonstrate the advantages of this approach.

Acknowledgements

Special thanks to my supervisor, Dr. Zezhong C. Chen. I really appreciate his enlightenment, encourage, support, and trust in me. Thanks to Conway Daly for his advice and for proof-reading my dissertation, and to Xiaohong Cong for giving me a lot of good advice. I also thank Concordia University faculty and staff who provided assistance.

Montreal's kind people and quiet environment were also very helpful to my research.

Table of Contents

List of Figures

List of Tables

Chapter 1 Introduction

1.1 Computer Numerical Control (CNC) Machining

CNC is defined as a self-contained numerical control (NC) system for a single machine tool that uses a dedicated computer controlled by stored instructions in the memory to implement some or all of the basic NC functions [15]. CNC machining plays an important role in manufacturing industry. Unlike traditional machining methods, CNC machines can manufacture complex shape and high-precise parts, and most parts with complex shape are currently machined with CNC machine tools. For example, the body of the Ferrari 360 Challenge Stradale Car and the turbine blades of airplane engines are machined by CNC machining (see Figures 1.1 and 1.2). Usually CNC machining has higher machining efficiency than traditional machining. CNC machining has been widely used in the aeronautical, automotive, and injection mould/die industries.

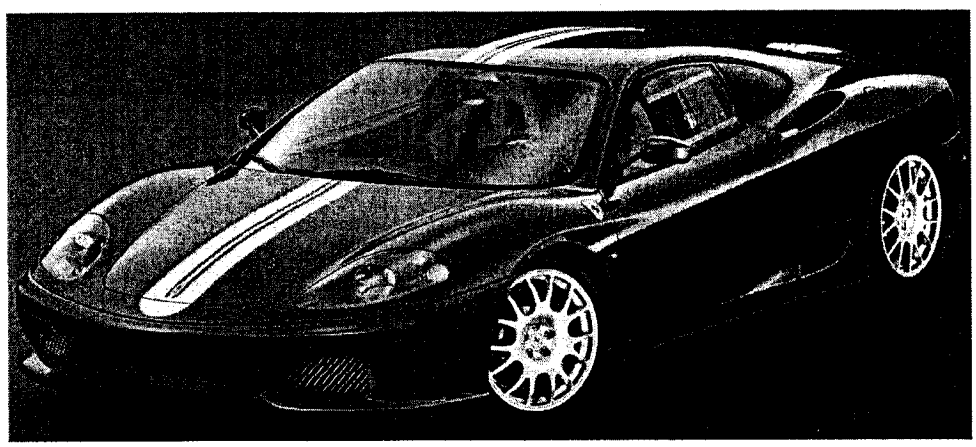

Figure 1.1 Ferrari 360 Challenge Stradale Car

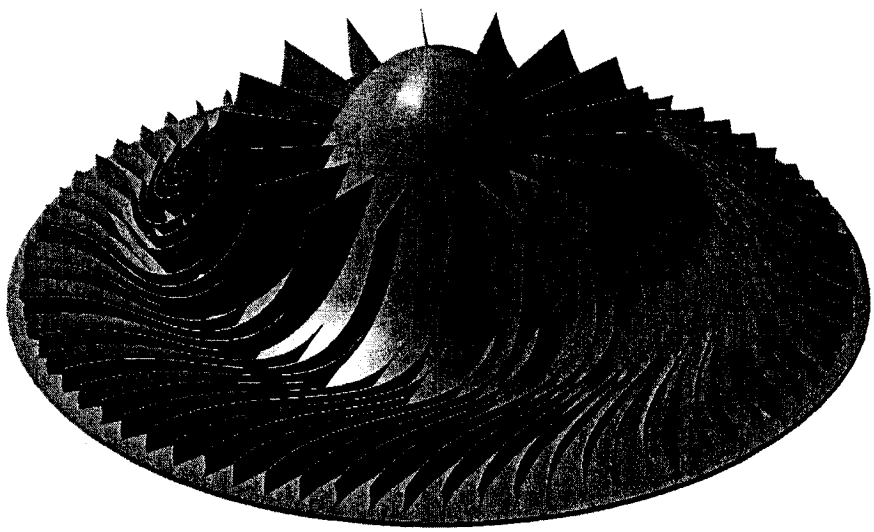

Figure 1.2 Impellers of an Airplane Engine

1.2 CNC Machining Strategies and CNC Machine Types

1.2.1 CNC Machining Process

Generally, the CNC machining consists of three steps: (1) rough machining, (2) semi-finish and finishing machining, and (3) grinding/polishing. Rough machining removes the excess stock material quickly to form a shape slightly larger than the part design, thus high machining productivity is its primary concern. Finishing machining

produces adequate quality surfaces by cutting the rough shape to the design. Better surface finishing requires less costly and labor-intensive manual polishing at the final stage. Adequate quality surfaces, less gouging, and minimum machining time are the objectives of the finishing machining. Different machining strategies and determination of machining parameters lead to variations in machining productivity and surface quality. A balance between surface quality and the machining time can be achieved by optimizing the feed rate of machining parameters.

1.2.2 CNC Machine Types

CNC machines are classified into three types: 2½-axis, 3-axis, and 5-axis CNC machines. The cutter on these machines includes three common types: ball, torus, and flat end-mill (see Figure 1.3). According to the different objectives of the rough and finishing machining, normally 2½-axis CNC machines are used for the rough machining, and 3-axis and 5-axis CNC machines are used for the finishing machining. In this section, the features of the 3-axis and 5-axis CNC machines are introduced; and the principles of selecting a CNC machine for parts machining are discussed.

Figure 1.3 Three Types of Common Milling Cutters [7]

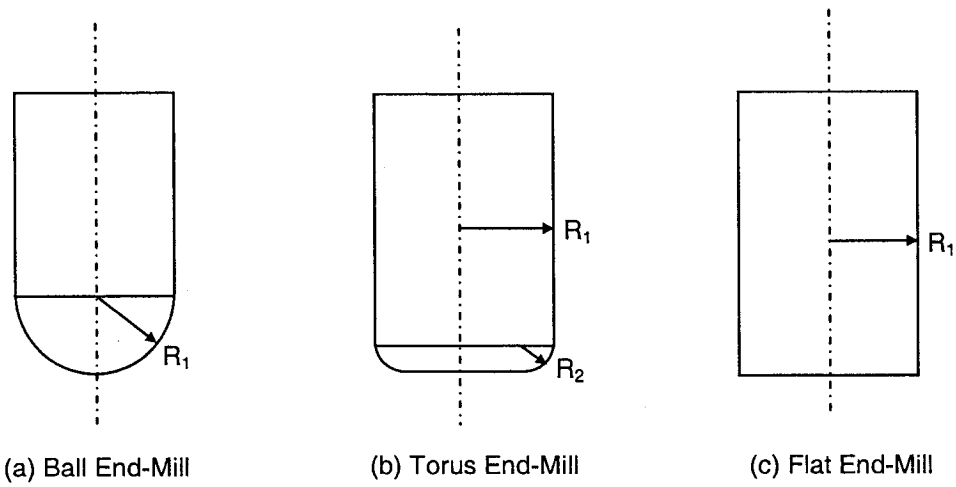

1.2.3 Two-and-a-Half-Axis CNC Machining

Two-and-a-half-axis CNC machining is often used for rough machining. The main feature of this type of machining is that the cutter motion in Z direction is not synchronized with the worktable motion in X and Y direction. In other words, the cutter remains the same height in Z direction when it cuts on a layer parallel to the worktable (X-Y plane). For the term 2½-axis CNC machining, "2" means the X- and Y-axis motions, and "½" means the Z-axis motion. Most of the 2½-axis CNC machining is carried out on 3-axis CNC milling machines.

Two-and-a-half-axis CNC machining is very efficient due to the highest material removal rate of the cutter and the rigid setup. This machining strategy is quick in roughly shaping a part. However, this machining is not applicable to the finishing machining of parts.

1.2.4 Three-Axis CNC Machining

Three-axis CNC machines are quite popular in the manufacturing industry due to their features, their advantages and high industrial demand. Three-axis CNC machining is exerted when a cutter of a 3-axis CNC machine moves along planned tool paths. This is because a 3-axis CNC machine executes three simultaneous motions including motions of the working table along X- and Y-axis and the cutter motion along Z-axis. Determined by the machine's architecture, the main feature of the machine is that the cutter orientation with respect to the part is locked after the part is fixed on the worktable. A 3-axis CNC vertical milling machine is shown in Figure 1.4; the cutter orientation is always in the vertical direction.

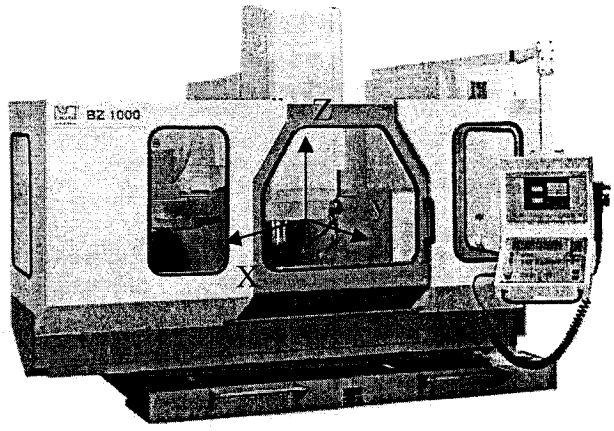

Figure 1.4 Diagram of a 3-Axis CNC Vertical Milling Machine

The 3-axis CNC machining feature enjoys some advantages. These advantages generally are (a) higher stiffness and rigidity of the machine prevents chatter in machining; (b) machine accuracy is high enough for finishing machining; (c) programming for tool paths in 3-axis CNC machining is manageable; and (d) the machine is affordable even for small businesses and its maintenance is not expensive[7]. Moreover, 3-axis CNC machining is the main metal working operation in the production process. Statistics show that besides the accurate prismatic parts, a majority of sculptured parts in the die/mould industry are made with 3-axis CNC machines. Therefore, 3-axis CNC machining is a major force in manufacturing industry.

While 3-axis CNC machines are popular, they are not universally able to mill all parts. In certain setups, the cutter cannot access some surface regions (or surface patches) of a part without interfering with the part. Three-axis CNC machining for some complex parts is only practical when all the surface patches to be machined can

be accessed by the cutter. This means that for some parts with complex shapes, a preferred solution is 5-axis CNC machining.

No matter which CNC machining method is adopted, the main machining parameters: spindle rate, feed rate, and depth of cut should be determined properly. Academic and industry researchers have been working for decades to find a way of determining the optimal machining parameters, because these parameters of CNC machining significantly influence part machining time, part surface quality, and tool life. The main objective of this work is to find an approach to determine feed rates in CNC profile milling. The following section provides a literature review of the proposed approaches on optimal machining parameters determination.

1.3 Related Work on Optimal Machining Parameters Determination

In mechanical parts machining, cutting efficiency, part accuracy and finish, and tool life are the major concerns. Higher cutting efficiency can reduce manufacturing costs, better part accuracy and finish means higher part quality, and longer tool life can save tooling expenses. Optimal machining parameters can significantly improve cutting efficiency and part quality. Considerable research has been conducted on the main machining parameters such as spindle speed, feed rate, and depth of cut. Unfortunately, a breakthrough has not been achieved since the problem is very complicated to address.

Currently spindle speed and depth of cut are determined based on machining handbooks according to the workpiece material, tool size and the nature of the tool material. After spindle speed and depth of cut are determined mechanically, the human

factor is at work in feed rate determination, when the machinist makes judgments based on his or her work experience. Such determined feed rate is quite conservative (which means lower than the peak efficiency) and does not take full advantage of all the possible cutting force variations in machining the whole part, and the machining time is long. The surface finish of the part is inconsistent, resulting in changes in the cutting force. On the contrary, the feed rate doesn't necessary to be set at the highest. At high rates, the tool can wear out too quickly or even break down, when the tool is overloaded at some location. Another negative factor is that the surface quality is reduced if the feed rate is set too high [9]. To achieve maximum efficiency, the feed rate should be adjusted simultaneously according to the variation of cutting force for the optimal machining effects.

1.3.1 On-Line and Off-Line Approaches to Feed Rate Determination

The optimal feed rate should be determined based on the part and tool material, cutting force, and depth of cut. The proposed approaches on feed rate determination can be broadly classified into on-line and off-line methods. The on-line approaches utilize force/torque sensors on tools to measure the cutting force/torque at the time of real machining and adjust the feed rate based on the varying cutting force/torque. However, the control system and sensors of the on-line approaches are quite expensive, so they are not widely used in industry. On the other hand, the off-line approaches predict cutting force according to cutting force models and set different feed rates at different locations. To determine the optimal feed rate, the current off-line approaches interpolate the experimental machining data to calculate the cutting

force and find the proper feed rate [4]. However, the results are not smooth and the predicted cutting force can not be determined reasonably and accurately.

1.3.2 Cutting Force Model and Feed Rate

The aim of the generic and intelligent approach of feed rate determination is to improve machining efficiency and part quality. Adjusting the feed rate necessarily changes the cutting force. The major technical challenge is how to find the mathematical relationship between the cutting force and the machining parameters such as feed rate, axial depth of cut, and radial depth of cut.

Many researchers have addressed feed rate determination from different perspectives. In traditional metal cutting theory, the cutting force is the key parameter in determining the kinetic and kinematical performance between the cutter and the machined surface. There are two categories of cutting force models: the infinitesimal flute model and the mean cutting force model. The infinitesimal flute model is very sensitive to its parameters. It is not easy to obtain the exact geometry of infinitesimal flutes from the cutters, and the dynamics of infinitesimal flutes is not clearly understood. The mean cutting force model is based on the material removal volume (MRV) or material removal rate (MRR). Although the calculation procedure is relatively simple, the mean cutting force model does have a drawback - it is unable to catch instantaneously the changes in cutting force [3].

An approach proposed by Bae, *et al.*, (2003) [4] is a simple cutting force regularization method to adjust feed rates for pocket machining. This approach first calculates the cutter engagement angle to measure the chip load in two dimensions

and then derives the relationship between the cutter engagement angle and the radial depth of cut. Next it builds up a simplified cutting force model based on the machining data in a cutting experiment with a tool dynamometer. Finally a method of automatic feed rate adjustment is used. This approach is more stable than the infinitesimal flute model and more accurate than the mean cutting force model. But since the axial depth of cut is not taken into account, the approach could not be applied when different axial depths of cut are used in CNC machining. There is another disadvantage due to the fact that the cutting force model is constructed by interpolating the experiment data with a Bezier surface. The Bezier surface is prone to fluctuation, which means the model can not represent the correct cutting force function in the local waving patch.

A different approach to feed rate determination can be found in the work of Baek, *et al.*, (2001) [5], which shows how to improve part quality by using the optimal feed rate, adopting the surface roughness model. The approach examines the variation of the feed rate based on the surface roughness model, while analyzing the dimensional accuracy in a face milling operation. Using a bisection method, the proper feed rate can be selected to provide a maximum material removal rate under the given surface roughness constraint. However, when applying a bisection method to a nonlinear system, it was very difficult to find the proper feed rate.

An approach of feed rate optimization for ball end milling, considering local shape features, is proposed by Lee, *et al.*, (1997) [23]. That paper studies a feed rate optimization program developed from the relationship between optimal feed rate and local shape features. Local shape features are classified as plain, upward ramp,

downward ramp, contour, convex corner and concave corner. They are all recognized by comparing NC codes of neighbouring points. A database for stable cutting conditions of zinc base alloy is established through various experiments with different local shape features.

Off-line feed rate scheduling using virtual CNC based on an evaluation of cutting performance is proposed by Ko, *et al.*, (2003) [21]. That approach presents an advanced technology to determine automatically the optimum feed rates for two-and-a-half-axis CNC machining, without requiring the expertise of a machinist or the information contained in a machining data handbook. An analytical model for off-line feed rate scheduling is formulated to improve productivity and machining accuracy. Using that method, it is possible to regulate the cutting force, which drastically improves the overall form accuracy of the machined surface. The approach is not applicable to three-axis CNC machining.

Bailey, *et al.*, (2002) [6] propose a generic simulation approach of multi-axis machining for model calibration and feed rate scheduling. That paper shows how a modeling methodology can be applied for feed rate scheduling in an industrial application. Based on the predicted instantaneous chip load and a specified force constraint, feed rate scheduling is utilized to increase the metal removal rate. The feed rate scheduling implementation results in a 30% reduction in machining time when applied to an airfoil-like surface.

Ko, *et al.*, (2003) [20] propose an approach of off-line feed rate scheduling for 3D ball-end milling using a mechanistic cutting force model. Their work uses an

analytical model of off-line feed rate scheduling to obtain an optimum feed rate for 3D ball-end milling. Off-line feed rate scheduling is presented as an advanced technology, regulating the cutting force in terms of the cutter's teeth and the feed rate. The feed rate changes with the variation of the uncut chip thickness. To increase the accuracy of off-line feed rate scheduling, the size effect phenomenon is considered in the cutting coefficient model.

W. L. R. Ip (1998) [17] presents a fuzzy-based strategy for material removal optimization, applied to sculptured surface machining with ball-nosed cutters. His approach compensates the variations of cutting speed caused by changes of gradient on the sculptured surface. In his approach, a constant cutting force is maintained by adjusting the feed rate for each cutting point by considering other machining parameters, such as tool life and surface gradient. The fuzzy-based approach can also give faster computer-generated results than the normal heuristic methods. In addition, the fuzzy approach has an attractive simplicity.

Research on predicting a cutting force is found in the work of Liu, *et al.*, (2002) [24]. The authors present an improved theoretical dynamic cutting force model for peripheral milling, which includes the size effect of unformed chip thickness, the influence of the effective rake angle and the chip flow angle. The paper suggests ways to select the cutter size and the cutting parameters for a good distribution of the cutting force, while reducing machining error and keeping a high productivity.

1.4 Objectives and Outline of This Work

This thesis includes seven chapters covering three main topics:

- a new and generic approach to determine machining parameters,
- a multiple-input-and-single-output (MISO) fuzzy system which has three inputs and a single output,
- a programming system for determination of proper feed rate based on the geometric features of a part.

Chapter one introduces CNC machining, CNC machining strategies, and CNC machining parameters determination methods. The literature review has been done, and the objectives of this work are provided. The statement of chapter two lays the theoretical preparation for the new CNC machining feed rate determination approach. The two-dimensional chip load model is introduced, and a machining parameter database is presented. Chapter three discusses a fuzzy rule-based system to predict cutting forces at every cutter location based on the radial and axis depth of cut, and the feed rate. Chapter four addresses the methods to find the maximum cutting force. A new approach of finding maximum cutting force based on geometry is introduced. Chapter five addresses the procedure used to identify the geometric features of the part, to calculate the engagement angles for the geometric features, and to find the proper feed rates. Chapter six applies this approach to an example part for profile milling, and the results are simulated with CATIA CAD/CAM system to demonstrate the advantages of this approach. A programming system for determination of proper feed rate based on the geometric features of a part is also described in this chapter. Chapter seven contains the summary and contributions of this work.

Chapter 2 A Machining Parameter Database for CNC Profile Milling

2.1 Terminology and Concepts in CNC Machining

To make this thesis clear, several common terms in CNC machining are introduced. Suppose a part is machined with a ball end-mill on a 3-axis vertical CNC machine, in which the working table moves along X- and Y-axis and the cutter along Z-axis.

Figure 2.1, showing a design surface and its machined surface, illustrates the following terms:

- A cutter contact (CC) point: a point on the surface at which the cutter touches the surface in machining. The cutter machines the surface exactly at the CC points [7].
- A tool path of cutter contact points: a curve on the surface through a number of the CC points which the cutter passes in one successive machining [7].
- Raw stock: a stock of a workpiece prior to machining.
- Preformed surface: the shape of a machined surface being processed before a particular machining operation.

- Postformed surface: the shape of a machined surface after a particular machining operation.
- Design surface: an ideal shape of a surface specified by designers.
- Stock allowance: the distance between a preformed surface and a design surface.
- Depth of cut: the distance between a preformed surface and a postformed surface.
- Machining tolerance: the allowed deviation of the actual machined surface from the postform surface [10].

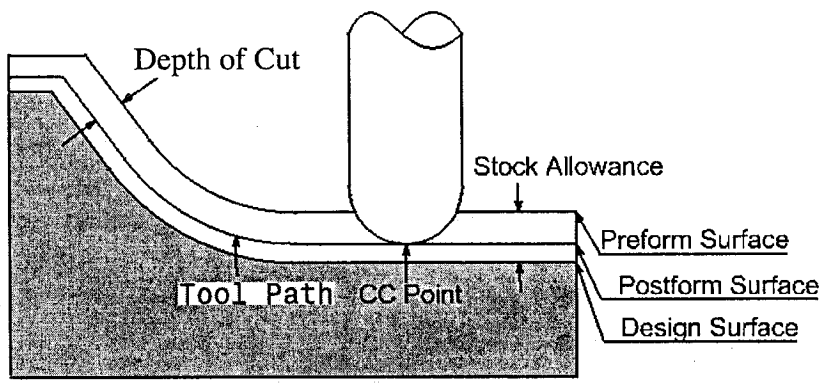

Figure 2.1 Some Basic Definitions in CNC Machining

After some basic CNC milling machining concepts are defined, one important concept in CNC machining milling - tool path topology - should be introduced. CNC milling machining is a milling process, in which a sequence of CC points is traced by milling cutters. The pattern of 'tracing' is called the tool path topology. There are four types of tool path topology patterns: (1) serial pattern, (2) radial pattern, (3) strip pattern, and (4) contour pattern (see Figure 2.2) [10].

Generally, both the serial pattern and radial pattern are for machining an area, and the contour pattern is for cutting a vertical or slant wall. In this work, the contour pattern tool path is taken in CNC profile milling.

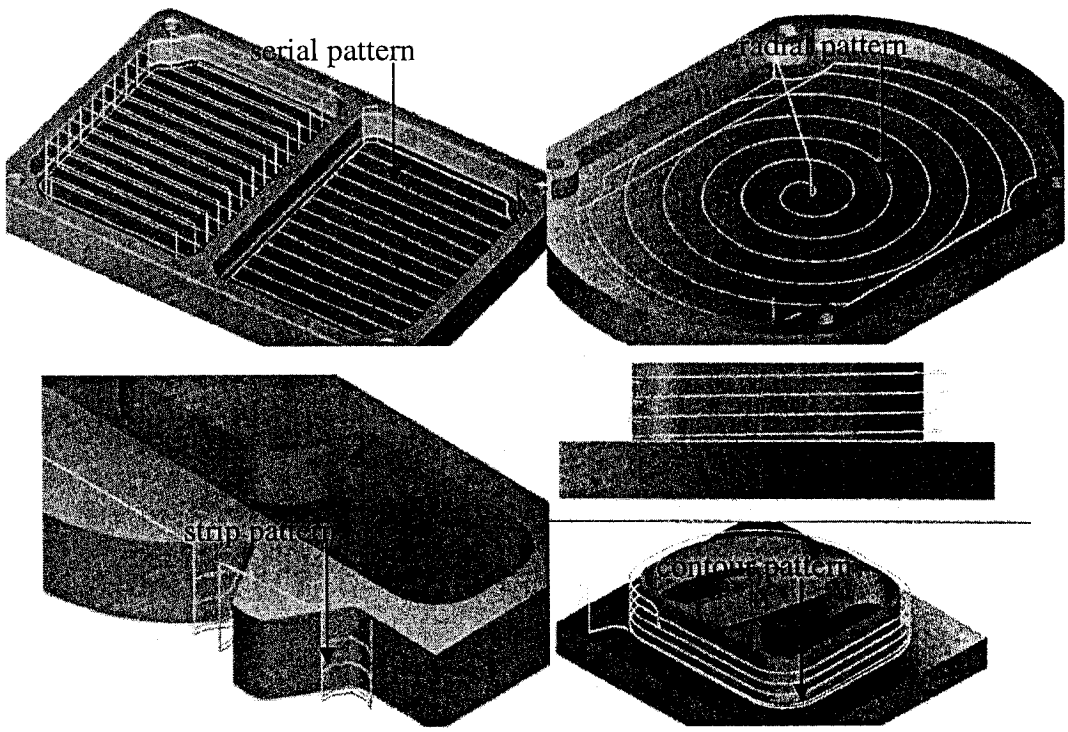

Figure 2.2 Tool Path Topology

2.2 CNC Profile Milling

Flat end mills are often used in profile milling of a part and machines the part along its profile. The depth of cut of the profile milling includes axial and radial depths of cut. The axial depth of cut is the thickness of removed material along the tool's axis direction, and the radial depth of cut is the thickness of the removed material by the tool side [9]. They are shown in Figure 2.3.

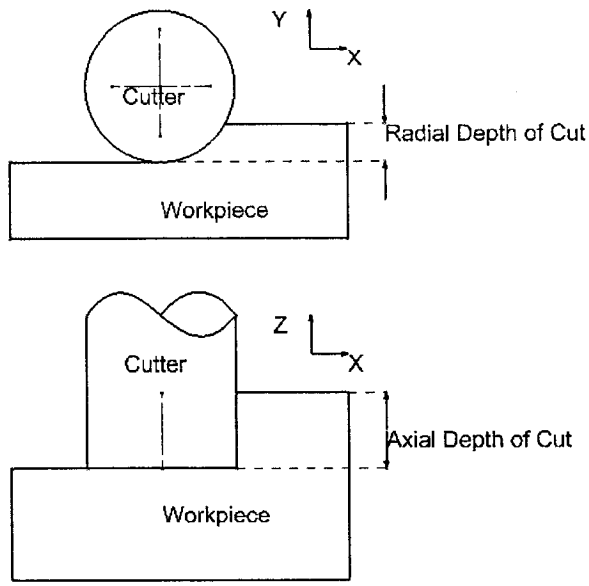

Figure 2.3 Radial Depth of Cut and Axial Depth of Cut

Generally, due to the difference in geometric shapes along the part profile, the cutter's chip load is different when it cuts in the geometries, so is the cutting force. A part profile can consist of (1) straight lines, (2) concave and convex shape formed by line segments (called concave and convex turns), and (3) concave and convex shape formed by curves (called concave and convex curves). The cutter's chip load changes when the tool is located at different points. The cutter's chip load is larger when the tool is working on a concave shape than when it is operating on a convex shape. The cutter's chip load is different from point to point if the tool cuts a curve. The chip load is determined by the axial and radial depth of cut. The chip load can be measured simply by engagement angle, which will be introduced in the following section.

2.3 Chip Load Model

In finish machining, any change in the surface shape could result in variation of chip load. This is not good for the surface quality of the machined part [10]. The topic to be discussed in this section is two-dimensional models for chip load estimation.

Figure 2.4 shows a part being machined with a flat end-mill, with the part profile presented in a top view. In order to simplify the analysis, all the dimensions are scaled down to the cutter radius, so the cutter radius in the model is 1. For a given value of nominal radial depth of cut (δ_0), the nominal engagement angle (γ_0) of the cutter at the linear region is given by

$$\gamma_0 = \cos^{-1}(1-\delta_0) \qquad 0 \le \delta_0 \le 1 \tag{2.1}$$

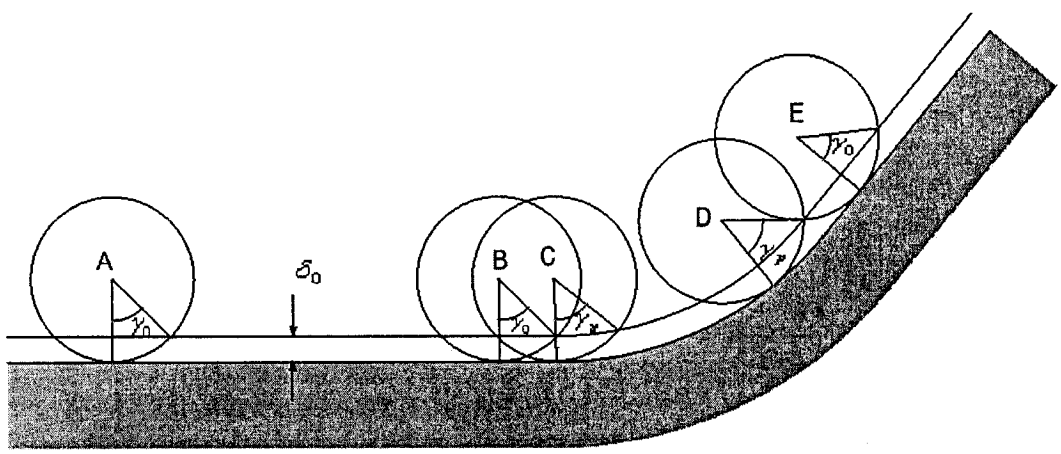

Figure 2.4 Two-D View of Flat End Milling Process

As depicted in Figure 2.4, the cutter engagement angle γ starts to increase from the point B, and reaches to its peak value γ_p at the point C.

The function of the cutter engagement angle γ with respect to different locations is sketched in Figure 2.5. Between AB and CD, the engagement angle remains the same,

and it increases from B to C. The effective radial depth of cut δ_e (the equivalent value of δ at the linear region for a given value of γ) is expressed in terms of γ as follows:

$$\delta_e = 1 - \cos\gamma \tag{2.2}$$

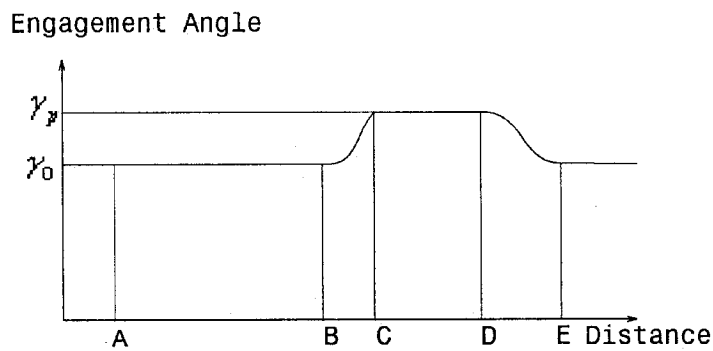

Figure 2.5 Cutter Engagement Angles

Either the cutter engagement angle γ or the effective radial depth of cut δ_e can be used as a measure of chip load [10].

A practical approach to accommodating the chip load variation of Figure 2.5 is to (1) split the block AC into two at the point B and (2) assign a reduced feed rate to the interval BC based on the peak value of chip load. But in the case of the convex block, an increased feed rate should be used. That is because the effective radial depth of cut at the convex region is less than the effective radial depth of cut at the linear region for a given value of γ [10]. In this work, feed rate determination depends on the changes in chip load.

Generally, the chip load is determined by the radial and axial depth of cut, and the radial depth of cut can be calculated by the engagement angle. If the engagement angle is larger, the chip load is bigger and the cutting force is greater. When feed rate is increased,

the cutting force is increased. The cutting force is a function of the radial and axial depth of cut and the feed rate. But obviously, the function is not linear. The functional relations could be determined either from actual cutting experiments or based on the metal cutting theory. In this work, the function is established from actual cutting experiments.

2.4 A Machining Parameter Database

The relationship among the cutting force, the depth of cut, and the feed rate is very complicated. Since it varies with such factors as the workpiece material, cutter material and size, and the machine tools, it's very difficult to establish a generic equation of these functions. But building a machining parameter database to represent the relationship can determine the proper feed rate.

To build this database, first the axial depth of cut is fixed, and a part is machined with different radial depths of cut and different feed rates. The cutting forces are tested and recorded in each different case. Then the axial depth of cut is changed and the same steps are repeated. After several iterations, a machining parameter database is built. The following table presents a machining parameter database. (It should be noted that numbers for the 3 *mm* axial depth of cut have been determined through machine experiments, but numbers for the other axial depths of cut have not been subject to experimentation and are provided only by way of illustration). For the 3 *mm* axial depth experiment, the cutter used was a high-speed steel flat end-mill having two flutes with the diameter of 10 *mm*, and the workpiece material was pre-hardened steel [9].

Table 2.1 Machining Parameter Database

Axial Depth of Cut is 3 *mm*					
Cutting Force (N)		Feed rate (*mm/min*)			
		50	100	150	200
δ_e	0.1	3.49	5.27	6.52	7.05
	0.2	4.52	6.73	8.36	9.56
	0.3	5.20	7.72	9.75	11.55
	0.4	5.62	8.59	10.47	12.53
	0.5	5.88	9.14	11.45	13.62
	1.0	6.61	10.14	12.94	16.35
Axial Depth of Cut is 4 *mm*					
Cutting Force (N)		Feed rate (*mm/min*)			
		50	100	150	200
δ_e	0.1	4.65	7.02	8.69	9.40
	0.2	6.03	8.97	11.14	12.74
	0.3	6.93	10.29	13.00	15.40
	0.4	7.49	11.45	13.96	16.70
	0.5	7.84	12.18	15.26	18.16
	1.0	8.81	13.52	17.25	21.80
Axial Depth of Cut is 5 *mm*					
Cutting Force (N)		Feed rate (*mm/min*)			
		50	100	150	200
δ_e	0.1	5.82	8.78	10.86	11.75
	0.2	7.53	11.21	13.93	15.93
	0.3	8.66	12.86	16.25	19.25
	0.4	9.36	14.31	17.45	20.88
	0.5	9.80	15.23	19.08	22.69
	1.0	11.01	16.90	21.56	27.24
Axial Depth of Cut is 6 *mm*					
Cutting Force (N)		Feed rate (*mm/min*)			
		50	100	150	200
δ_e	0.1	6.98	10.54	13.04	14.10
	0.2	9.04	13.46	16.72	19.12
	0.3	10.40	15.44	19.50	23.09
	0.4	11.24	17.18	20.93	25.05
	0.5	11.76	18.28	22.89	27.23
	1.0	13.22	20.27	25.88	32.69
Axial Depth of Cut is 7 *mm*					
Cutting force (N)		Feed rate (*mm/min*)			
		50	100	150	200
δ_e	0.1	9.77	14.75	18.25	19.74
	0.2	12.65	18.84	23.40	26.76
	0.3	14.56	21.61	27.29	32.33
	0.4	15.73	24.05	29.31	35.08
	0.5	16.46	25.59	32.05	38.13
	1.0	18.50	28.38	36.22	45.77

In this database, four different feed rates (50, 100, 150, and 200 *mm/min*) are used. The six effective radius depths of cutting are selected as (0.1, 0.2, 0.3, 0.4, 0.5, and 1.0), where the maximum radial depth of cut is set as the cutter radius. Five axial depths of cut are selected as (3, 4, 5, 6, and 7 *mm*).

Chapter 3 Fuzzy Logical System of Cutting Force Prediction

3.1 Introduction

Once the machining parameter database has been built, it is possible to tackle the problem of predicting the cutting force. One approach to the question can be found through fuzzy logic system. It is an appropriate tool to represent and deal with imprecision, vagueness and fuzziness in the real world. In this work, fuzzy logical system is used to predict the cutting force. There are three main reasons. The first one is that the cutting force function of the depth of cut and the feed rate is nonlinear. The second is that the machining parameter database describes the relationship in a discrete way. The third one is that fuzzy logic system could represent the nonlinear function in an intelligent way.

3.1.1 Basic of Fuzzy Logic

Fuzzy logic is a superset of conventional (Boolean) logic that has been extended to handle the concept of partial truth - truth values between "completely true" and "completely false". Fuzzy logic is based on the fact that most modes of human reasoning, especially common sense reasoning, are approximate. [13].

In this work, a fuzzy logic system is applied because it is:

- conceptually easy to understand;
- flexible;
- tolerant of imprecise data;
- useful in identifying complexities;
- linked to the experience of experts;
- presented in natural language [14].

3.1.2 Fuzzy Inference Systems

Fuzzy inference is a process of mapping a given input to an output using fuzzy logic. The process of fuzzy inference involves membership functions, fuzzy logic operators, and if-then rules. The structure of a fuzzy inference system is shown in Figure 3.1. Fuzzy inference systems are also known as fuzzy-rule-based systems and fuzzy models. They have been successfully applied on fields such as automatic control, data classification, decision analysis, expert systems, and computer vision. There are two types of fuzzy inference systems: Mamdani and Sugeno. These two types of inference systems vary somewhat in the way outputs are determined [13]. In this work, Mamdani fuzzy inference system is used to establish a cutting force model.

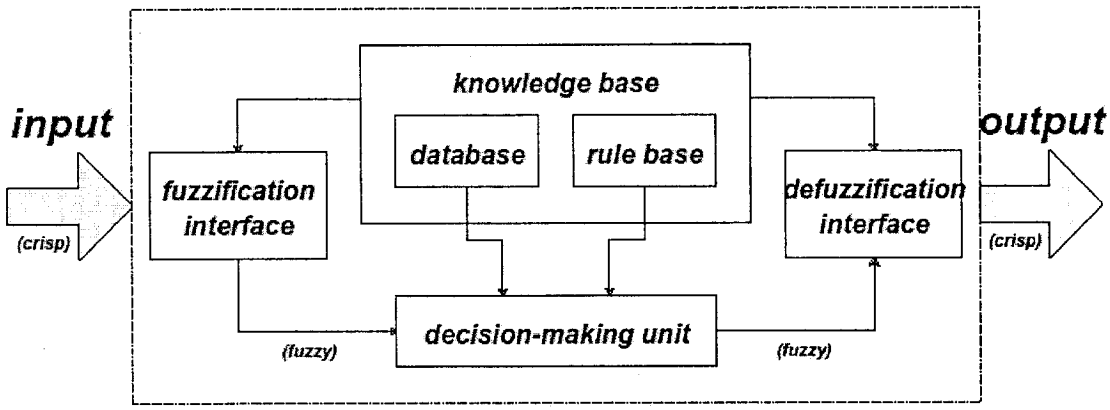

Figure 3.1 Fuzzy Inference System [31]

Mamdani fuzzy inference method is quite popular. The process of Mamdani fuzzy inference system includes five steps: (1) fuzzify input variables; (2) apply fuzzy operators (AND or OR) to antecedents; (3) implicate consequences from the antecedents; (4) aggregate the consequences across the rules; and (5) defuzzify the consequences for outputs [14]. Usually, step (1) is fuzzification interface. Step (5) is defuzzification interface. The five steps will be described in detail in the following.

Step 1. Fuzzify Inputs

The first step is to take the inputs and find out the proper fuzzy sets in each input domain. Then use their membership functions to determine the membership degrees to the fuzzy sets for each input. In this step, the inputs are crisp and vary within the discourse in the input domain. The membership degree varies from 0 to 1. When the membership of a fuzzy set equals to 1, the input is completely a member in the fuzzy set. When the membership of a fuzzy set equals to 0, the input is absolutely not in the fuzzy set.

Step 2. Apply Fuzzy Operators

If a given rule has more than one antecedent, the fuzzy operators are applied to the antecedents that represent the result of the antecedent of that rule. The input to the fuzzy operator is two or more membership values from fuzzified input variables. The output is a single number.

Usually, the AND operator is either min (minimum) or algebraic product function. The OR operator is either max (maximum) or algebraic sum function. For instance, the algebraic product and algebraic sum functions are defined in the following equations, respectively.

$$\text{Product}(a, b) = ab \tag{3.1}$$

$$\text{Sum}(a, b) = a + b - ab \tag{3.2}$$

Step 3. Apply Implication Method

Before applying the implication method, the rule's weight should be considered. Every rule is designated a weight - a number between 0 and 1. Generally this weight is 1.

Once proper weights have been assigned to each rule, the implication method is employed. In the implication process, the consequence is reshaped using a function associated with the antecedent [14]. The input for the implication process is a single number given by the antecedent, and the output is a fuzzy set represented by a

membership function. Usually, in this step, two methods are used: min (minimum) and algebraic product.

Step 4. Aggregate All Outputs

After decisions are made based on the results of testing all of the rules in a fuzzy inference system, the rules must be combined in some manner. Aggregation is an operation by which the fuzzy sets that represent the outputs of the rules are combined into a single fuzzy set. The input of the aggregation operation is the list of truncated output functions generated in the implication process for each rule. The output of the aggregation operation is one fuzzy set for each output variable.

Since the aggregation operation is commutative, the order in which the rules are executed is unimportant. Usually, three functions are used: max (maximum), algebraic product, and sum - simply the sum of each rule's output set.

Step 5. Defuzzify

The input for the defuzzification process is a fuzzy set - the aggregate output fuzzy set. There are situations where a crisp value is needed instead of this fuzzy set such as fuzzy control applications [13]. Therefore, the final step that converts the fuzzy set into a crisp value is needed.

The most popular defuzzification method is the centroid calculation, which finds the center of an area. Usually, there are five methods used: (1) centroid; (2) bisector; (3) middle of maximum - the average of the maximum value of the output set; (4) largest of maximum; and (5) smallest of maximum.

3.2 A Fuzzy Logic System

To represent the machining parameter database (Table 2.1), a system of fuzzy logical inference is employed. The system consists of membership functions of the fuzzy variables, a rule base, fuzzy reasoning and defuzzification. The structure of the fuzzy system for a machining parameter database is shown in Figure 3.2; RDC denotes the radial depth of cut and ADC stands for the axial depth of cut.

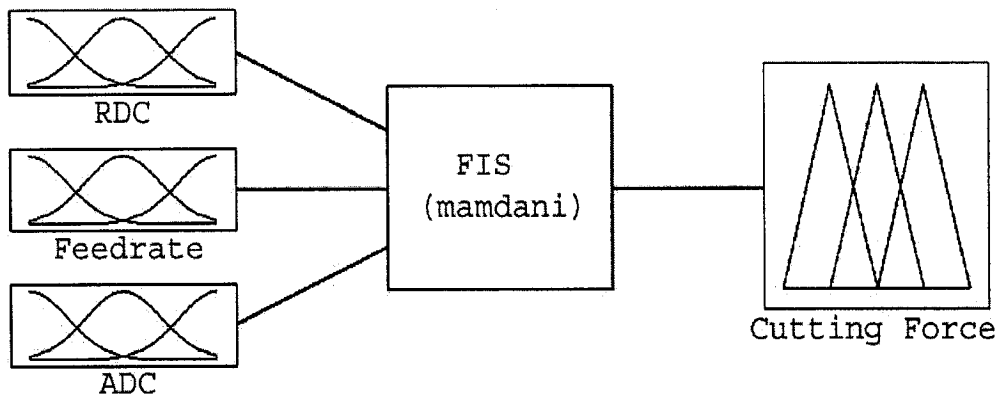

Figure 3.2 Structure of the Fuzzy Inference System

3.2.1 Fuzzy Membership Functions

In generating a fuzzy set for a fuzzy variable, the first step is to define a membership function for each fuzzy variable. The membership function of the fuzzy variable is chosen among several functions which are defined within the variable interval, and the range of each membership function is between zero and one. Different membership functions result in different output, and the selection of the membership functions depends on individual experience.

In general, the following membership functions are used in a fuzzy system: triangular-shaped; Gaussian; single sigmoidal; paired sigmoidal; generalized bell; and s-shaped. In this work, the Gaussian membership function is used. However, the

other membership functions also present interesting possibilities and are worth a brief examination.

(1) Triangular-Shaped Membership Function

The triangular-shaped membership function has three parameters: a, b, c. The "feet" of the triangle are a, c and the "head" of the triangle is b [14]. The mathematical formulae of the function are given in Equation 3.3 and the function figure is shown in Figure 3.3:

$$f(x;a,b,c)=\begin{Bmatrix} 0 & x\le a \\ \dfrac{x-a}{b-a} & a\le x\le b \\ \dfrac{c-x}{c-b} & b\le x\le c \\ 0 & c\le x \end{Bmatrix} \tag{3.3}$$

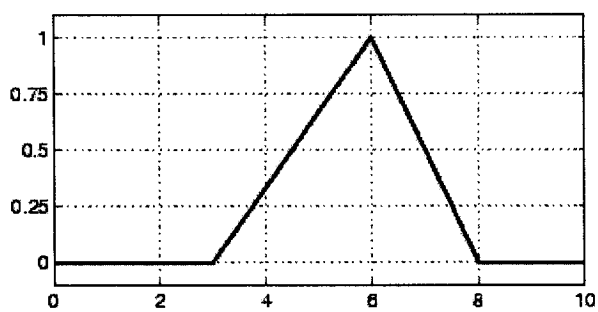

Figure 3.3 Triangular-Shaped Membership Function [14]

(2) Gaussian Membership Function

The Gaussian membership function has two parameters, σ, which represents the slope, and c, which is the peak of the slope. It is given by:

$$f(x;\sigma,c)=e^{\frac{-(x-c)^2}{2\sigma^2}} \tag{3.4}$$

The function figure is shown in Figure 3.4

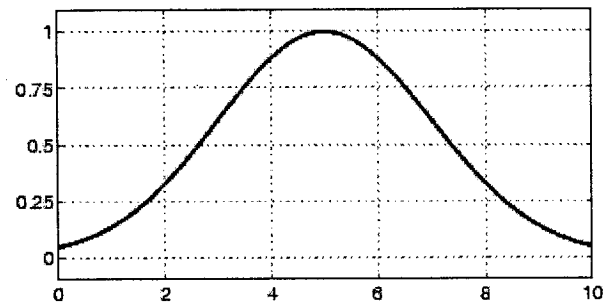

Figure 3.4 Gaussian Membership Function [14]

(3) Sigmoidal-Shaped Membership Function

The sigmoidal-shaped membership function has two parameters, a and c, and the given equation is:

$$f(x;a,c) = \frac{1}{1+e^{-a(x-c)}} \tag{3.5}$$

The function is plotted in Figure 3.5.

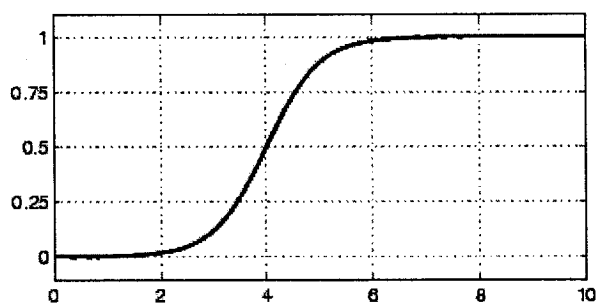

Figure 3.5 Sigmoidal-Shaped Membership Function [14]

3.2.2 Four Fuzzy Variables Membership Functions

Since the Gaussian membership function is smoother than the triangular function, the Gaussian function is adopted to calculate the membership for a fuzzy variable, the radial depth of cut. This function is plotted in Figure 3.6. The parameters of the

membership functions of the radial depth of cut are presented in Table 3.1. The three membership functions reach their maximums at different values of the radial depth of cut, and the membership functions are identified accordingly as low, medium, and high. Similarly, the Gaussian function is adopted as the membership functions for both the axial depth of cut and the feed rate. The membership functions for the axial depth of cut are also identified as low, medium, and high, while those for the feed rate as slow, medium, and fast. These membership functions for the feed rate and the axial depth of cut are plotted in Figure 3.7 and 3.8, respectively. The feed rate interval is specified between 50 and 200 *mm/min*, and the axial depth of cut is from three to seven millimeters. The parameters for membership functions of the feed rate and the axial depth of cut are presented in Table 3.2 and 3.3, respectively.

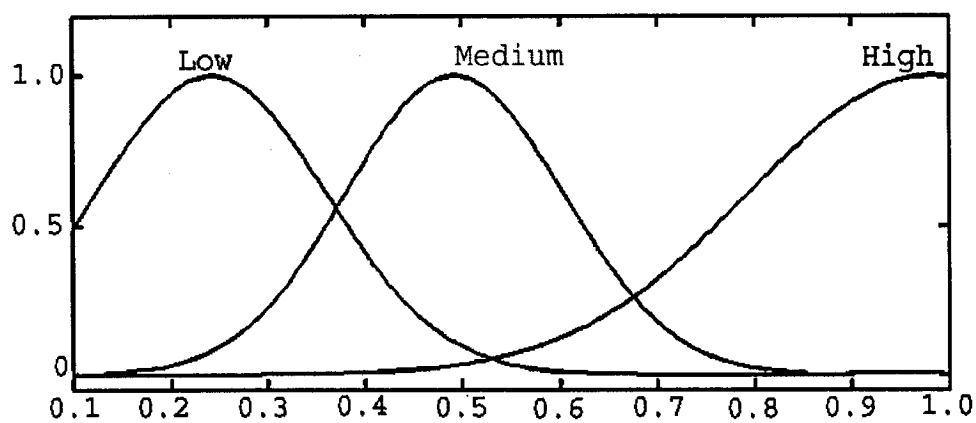

Figure 3.6 Membership Functions of the Radial Depth of Cut

Table 3.1 Parameters for Membership Functions of the Radial Depth of Cut

	Low	Medium	High
σ	0.119	0.112	0.187
C	0.242	0.492	0.981

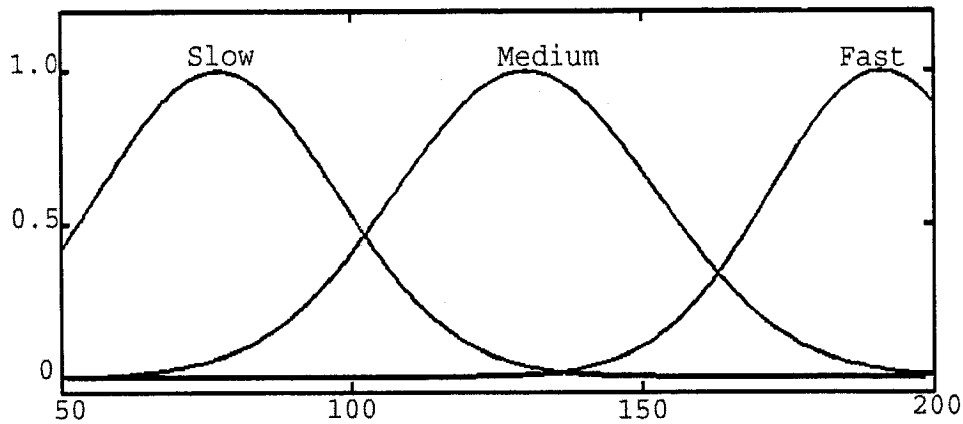

Figure 3.7 Membership Functions of the Feed Rate

Table 3.2 Parameters for Membership Functions of the Feed Rate

	Slow	Medium	Fast
σ	20.4	22.3	19.1
C	77.0	130.0	191.0

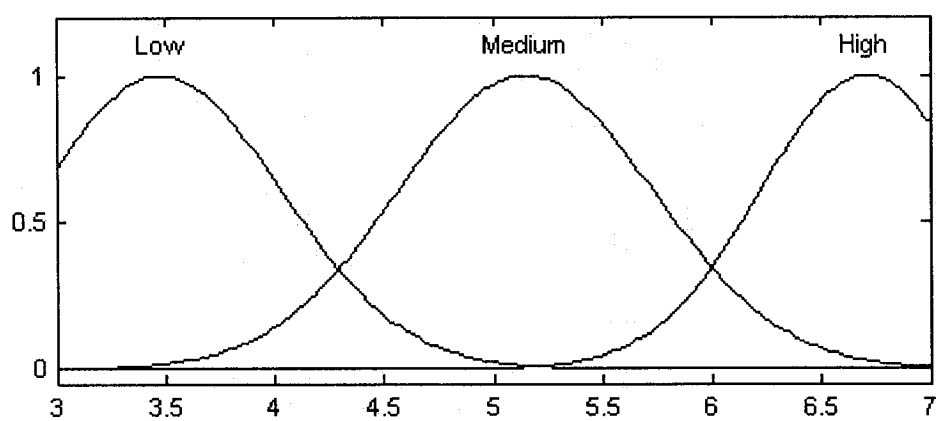

Figure 3.8 Membership Functions of the Axial Depth of Cut

Table 3.3 Parameters for Membership Functions of the Axial Depth of Cut

	Low	Medium	High
σ	0.555	0.584	0.488
C	3.480	5.147	6.707

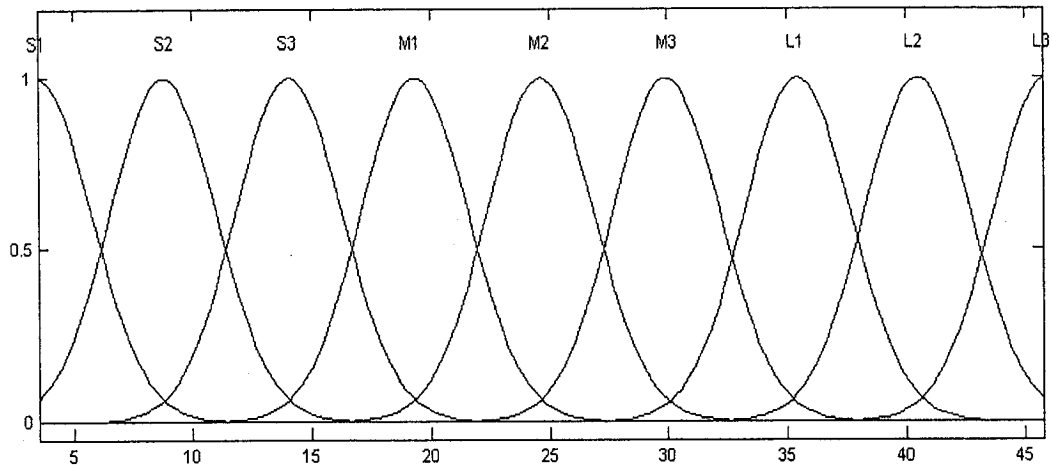

Figure 3.9 Membership Functions of the Cutting Force

Table 3.4 Parameters for Membership Functions of the Cutting Force

	σ	C
S1	2.241	3.490
S2	2.245	8.776
S3	2.234	14.070
M1	2.245	19.340
M2	2.250	24.630
M3	2.245	29.930
L1	2.232	35.420
L2	2.249	40.470
L3	2.252	45.910

Gaussian function is used to define the membership function for the output. These nine output-related membership functions of the cutting force are defined and shown in Figure 3.9. The nine membership functions of the cutting force are identified as level one of small (S1), level two of small (S2), level three of small (S3), level one of medium (M1), level two of medium (M2), level three of medium (M3), level one of large (L1), level two of large (L2), and level three of large (L3). According to the machining parameter database, the cutting force interval is within the range of 3.49 to 45.77 *N*. The parameters for the membership functions of the cutting force are presented in Table 3.4.

3.2.3 Fuzzy Rules

A fuzzy rule base should be set up after the membership functions for the fuzzy variables have been defined. Generally the fuzzy rule in a rule base is expressed in the form of a logical statement, e.g. IF_THEN [12]. However, the fuzzy system discussed in this paper is more complicated. It has three inputs and single output, which falls into the category of a multiple-input-and-single-output (MISO) system. The logical operator AND is used to connect the three inputs to form an aggregated statement as a rule, and all the rules are in the form as IF_AND_AND_THEN. In this work, the min (minimum) function of the AND operator is used. Each input fuzzy variable has three different membership functions and the combination of the three fuzzy variables can compose twenty seven rules in this fuzzy system. The combination is listed in Table 3.5.

Table 3.5 Combination of the Membership Functions of Fuzzy Variables

Axial Depth of Cut is Low				
Cutting Force		Feed Rate		
		Slow	Medium	Fast
Radial Depth of Cut	Low	S1	S2	S3
	Medium	S2	S3	M1
	High	S2	M1	M2
Axial Depth of Cut is Medium				
Cutting Force		Feed Rate		
		Slow	Medium	Fast
Radial Depth of Cut	Low	S1	S3	M1
	Medium	S2	M1	M2
	High	S3	M3	L1
Axial Depth of Cut is High				
Cutting Force		Feed Rate		
		Slow	Medium	Fast
Radial Depth of Cut	Low	S2	S3	M2
	Medium	S3	M3	L1
	High	M1	M3	L3

Based on the Table 3.5, the twenty seven fuzzy rules can be composed as followings and form a rule base. For example:

- IF the axial depth of cut is low AND the radial depth of cut is low AND the feed rate is slow, THEN the cutting force is S1.
- IF the axial depth of cut is low AND the radial depth of cut is low AND the feed rate is medium, THEN the cutting force is S2.
- IF the axial depth of cut is low AND the radial depth of cut is low AND the feed rate is fast, THEN the cutting force is S3.
- (Other rules follow a similar pattern, such as:)
- IF the axial depth of cut is high AND the radial depth of cut is high AND the feed rate is medium, THEN the cutting force is M3.
- IF the axial depth of cut is high AND the radial depth of cut is high AND the feed rate is fast, THEN the cutting force is L3.

Each fuzzy rule in this rule base reflects a specific machining case with different machining parameters in principle and is correct with respect to the machining parameter database. For example, in the first fuzzy rule, when the radial depth of cut is low, the axial depth of cut is low, and the feed rate is slow, the cutting force is the level one of small. The first fuzzy rule describes a portion of the relationship between the cutting force and the fuzzy variables, and it is a qualitative interpolation of some data in the machining parameter database. With all the fuzzy rules, the machining parameter database is interpolated qualitatively and the function of the cutting force is fully represented. The fuzzy rule base is the heart of the fuzzy system and can be

used to predict the cutting force according to the three inputs, the axial depth of cut, the radial depth of cut, and the feed rate [31].

3.2.4 Cutting Force Prediction

The cutting force can be calculated using the fuzzy rule base instead of a close-formed equation. Determining the cutting force value using the fuzzy rule base is called fuzzy reasoning. Since the fuzzy rules reflect the actual machining correctly, the predicted cutting force is reasonable and the desired practical results can be achieved if some new values of the fuzzy variables are input.

In detail, two approaches, the min-min-max method and max-min-product method, are popular in the fuzzy reasoning process [17]. This work focuses on the min-min-max method, because there is a large amount of machining data available on this approach. In this method, the result of the fuzzy reasoning is obtained by using this method. However, the result of the fuzzy reasoning is not cutting force itself and can not be used directly. This value should be defuzzified into the predicted cutting force.

3.2.5 Defuzzification of Cutting Force

Defuzzification in this procedure is to map the fuzzy reasoning result to the actual cutting force. The centroid defuzzification is the most commonly used defuzzification in fuzzy systems because it is computationally simple and intuitively plausible [31]. In this work, the centroid defuzzification is used. The centroid defuzzification specifies the y^* as the center of the area covered by the membership function of B', that is,

$$y^* = \frac{\int_y y u_{B'}(y)dy}{\int_y u_{B'}(y)dy} \tag{3.6}$$

where $\int_y$ is the conventional integral. Figure 3.10 shows this operation graphically.

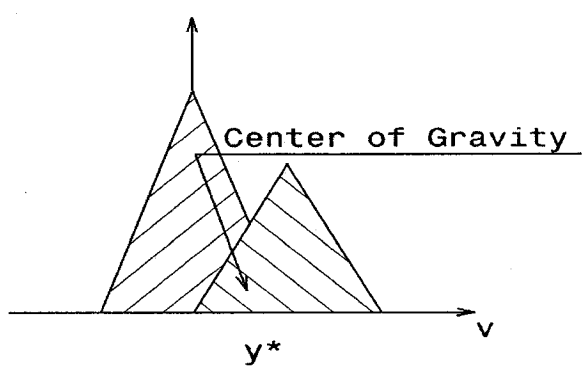

Figure 3.10 Graphical Representation of the Centroid Defuzzification.

The B' membership function can also be considered as the B' fuzzy set, which is the union or intersection of M fuzzy sets. A good approximation of above equation is the average of the centers of the M fuzzy sets, with the weights equal the heights of the corresponding fuzzy sets [31]. Figure 3.11 illustrates this operation graphically

for a simple example with M=2. Specifically, let y_l be the center of the l*th* fuzzy set and w_l be its height, the center average defuzzification determines y^* as

$$y^* = \frac{\sum_{l=1}^{M} y_l w_l}{\sum_{l=1}^{M} w_l} \tag{3.7}$$

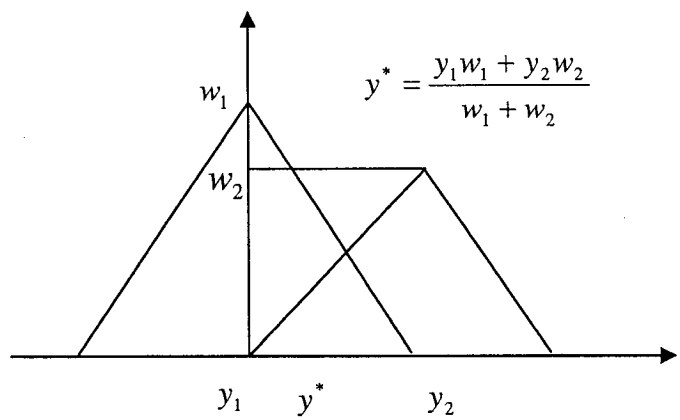

Figure 3.11 Graphical Representation of the Center Average Defuzzification

As a result, the relationship between the cutting force and the fuzzy variables in this fuzzy system is shown in Figure 3.12 and Figure 3.13.

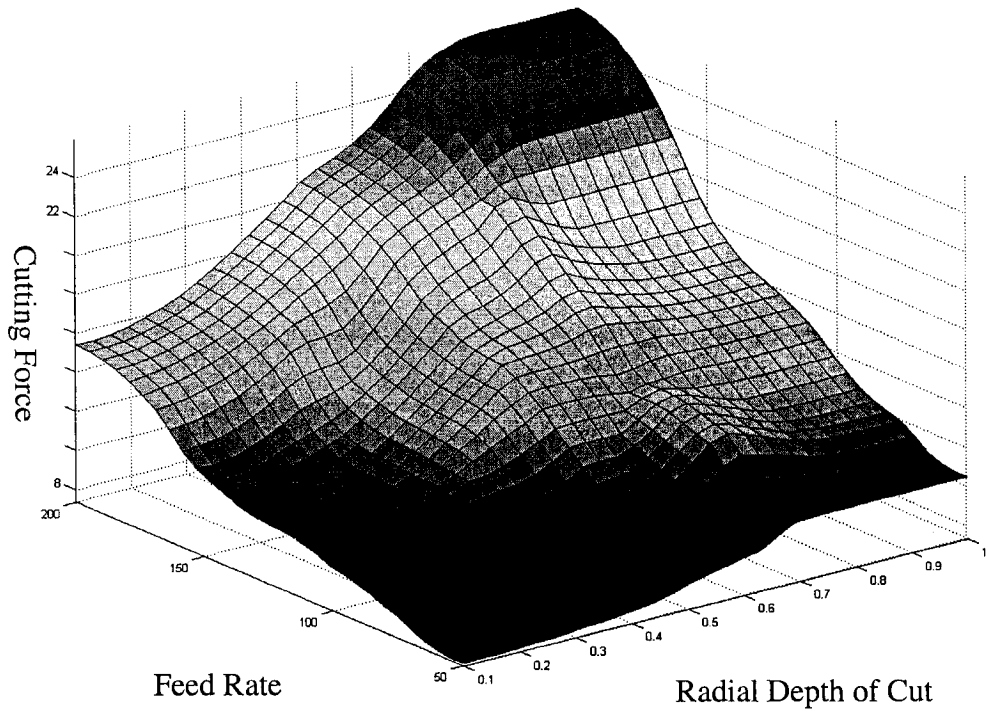

(a)

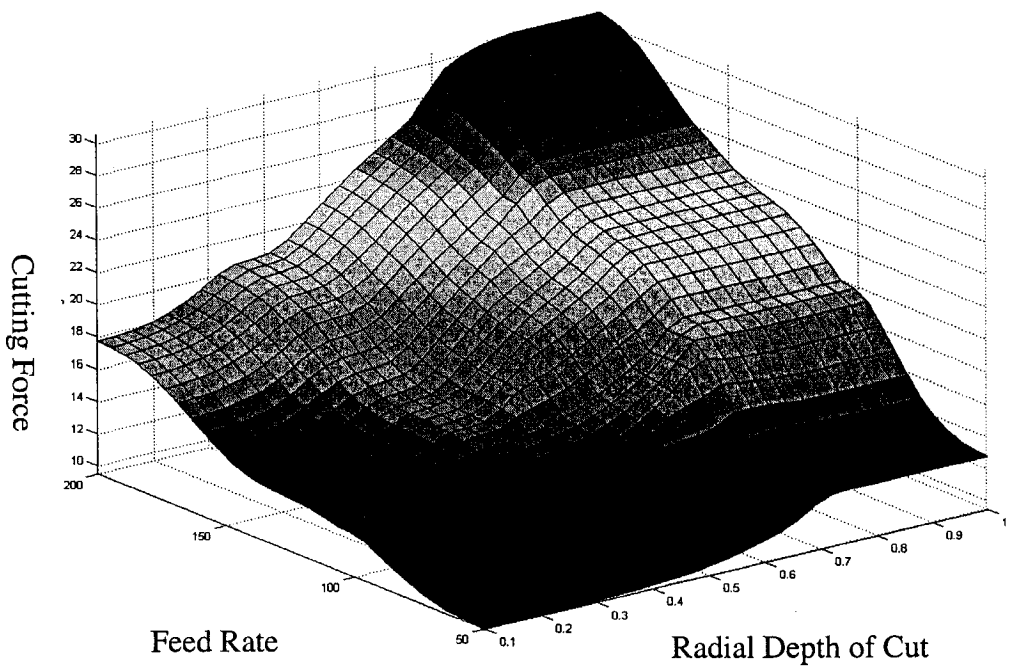

(b)

Figure 3.12 Surface of the Cutting Force Model (a) When the Axial Depth of Cut is 4.5 *mm*, (b) When the Axial Depth of Cut is 5 *mm*.

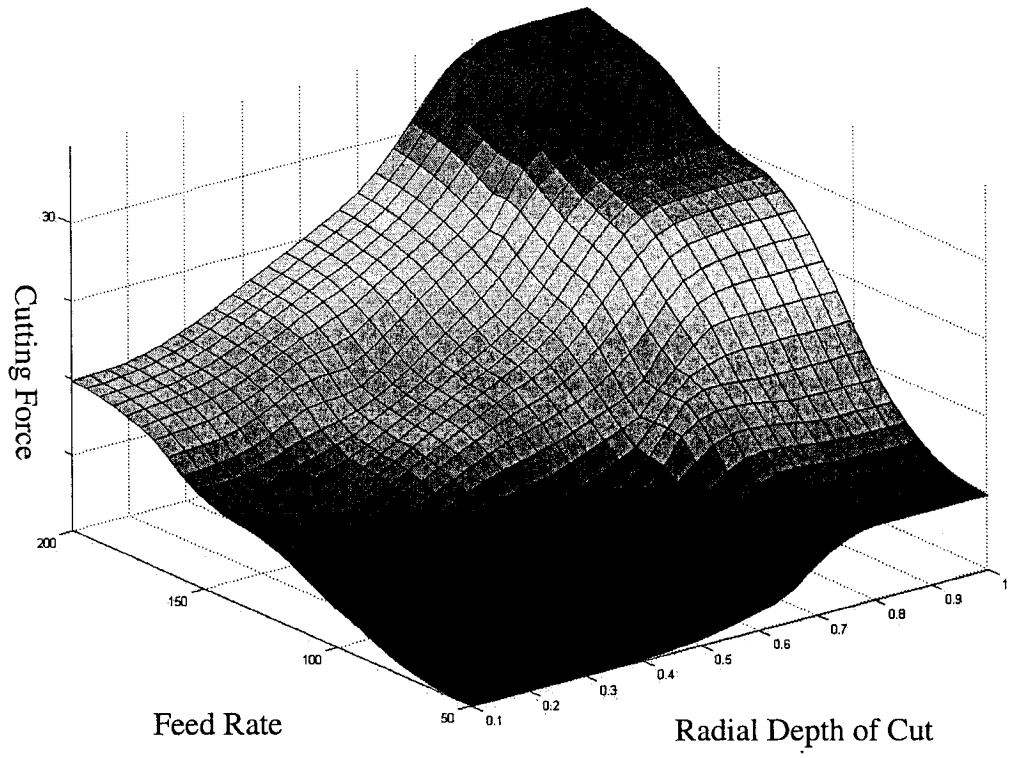

(a)

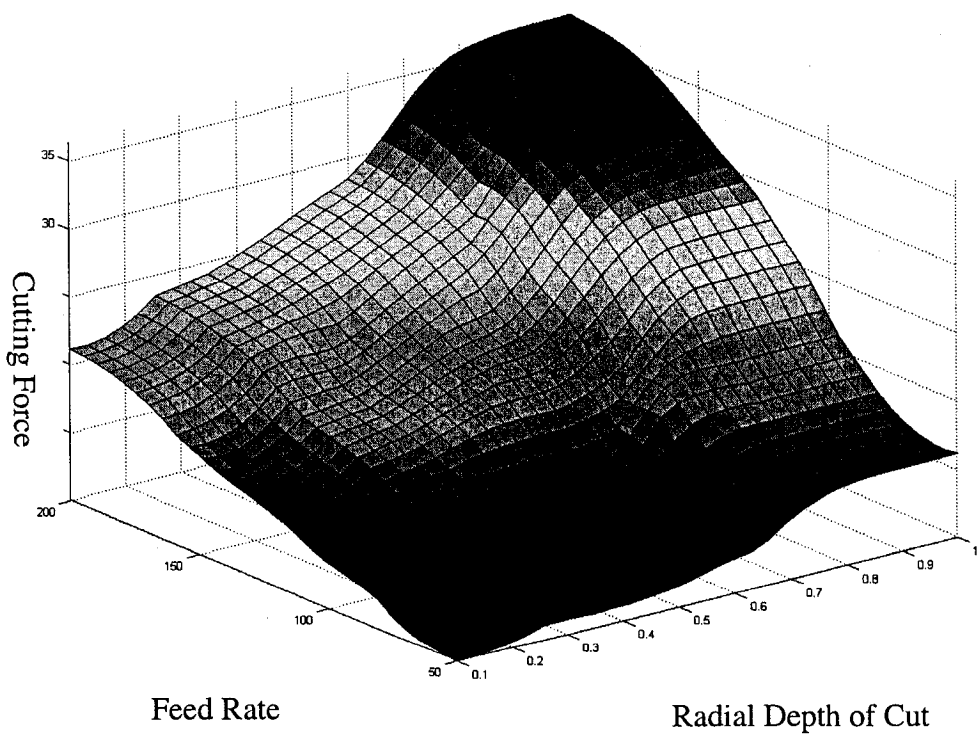

(b)

Figure 3.13 Surface of the Cutting Force Model (a) When the Axial Depth of Cut is 5.5 *mm*, (b) When the Axial Depth of Cut is 6 *mm*.

Chapter 4 Maximum Cutting Force Estimation

4.1 Introduction

The maximum cutting force in CNC machining is the cutting force limit, under which the tool can work in normal without severe wear and the CNC machine is free of chatter. If the cutting force imposed on the tool exceeds the limit, the tool will vibrate severely, causing worse surface quality and suffer wear greatly causing shortening tool life. Thus a machining with the maximum cutting force or over should be prevented. The maximum cutting force can be criteria in CNC machining. Feed rate is one of the factors influencing the cutting force. When feed rate is increased, the cutting force is increased nonlinearly, if the other factors are fixed. Up to the level where the cutting force reaches maximum, the feed rate can not be increased any more. To machine a part efficiently and safely, proper feed rates are so determined that the cutting force remain 80% of the maximum cutting force. Therefore, the maximum cutting force should be estimated before proper feed rates can be determined. Several cutting force methods for the maximum cutting force are reviewed in this chapter.

Usually the cutting force is presented as a function of radial depth of cut, axial depth of cut, and feed rate in milling. However, the cutting force is subject to many factors in metal cutting process. The factors are listed as following:

- Workpiece material – yield stress and hardness;
- Tool material – hardness, toughness, and thermal resistance;
- Tool geometry – rake angle, helix angle, number of flutes, and diameter;
- Machine tool characteristics – system stiffness (including the tool and spindle, machine structure, workpiece and fixtures), runout, cutting speed, and power [10].

Because the influence of machine tool characteristics is very difficult to evaluate, it is not taken into account in cutting force estimation.

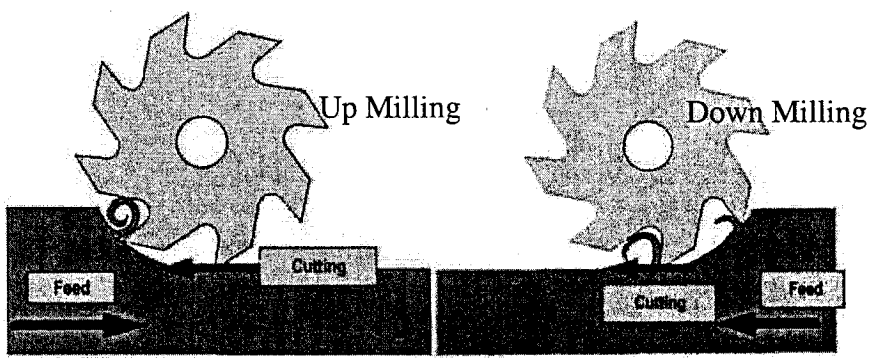

Figure 4.1 Up Milling and Down Milling

As illustrated in Figure 4.1, the cutting forces are different in the two milling conditions: up milling and down milling [1]. In up milling, the tool tends to be pulled close to the workpiece, which increases both the depth of cut and the cutting forces. Usually, up milling is adopted in rough machining, while down milling is used in finish machining [2]. In this work, two well-known cutting force models, the volumetric

cutting force model and the mechanistic cutting force model, are introduced and a new method based on the fuzzy logic system is proposed.

4.2 Volumetric Model

This cutting force model takes the chip geometry and the material removal rate (MRR) into account. The spindle power P should be given as follows:

$$P = K \cdot (MRR) \tag{4.1}$$

In this equation, K is the unit power consumption. The cutter power P is equal to the tangential cutting force F_t times the cutting speed V. So the tangential cutting force F_t is given by:

$$F_t = P / V = K \cdot (MRR) / V \tag{4.2}$$

The radial force F_r is calculated by:

$$F_r = K_r \cdot F_t \tag{4.3}$$

where K_r is a constant. The values of K and K_r depend on workpiece material, cutting tool geometry and cutting conditions. In CNC machining, MRR is given by:

$$MRR = \delta \cdot H \cdot c \tag{4.4}$$

where δ is the radial depth of cut, H is the axial depth of cut, and c is feed rate.

It is true that the volumetric force model is very simple to implement and can be useful to improve efficiency in the rough machining and semi-finish machining. The

maximum cutting force that is calculated using the volumetric force model is the average maximum cutting force. But the volumetric cutting force model has a major shortcoming: the calculated cutting force is average, not the instantaneous force. Force direction and cutter deflection direction are also unknown, so verification of surface accuracy is not possible. As a result, the cutting force model is not usually adopted in finish machining.

4.3 Mechanistic Cutting Force Model

The mechanistic cutting force model offers a way to overcome the main shortcoming of the volumetric cutting force model, its inability to calculate the instantaneous cutting force [1]. In milling machining, the instantaneous chip thickness (h) varies periodically if the cutter flutes are taken into consideration. The instantaneous chip thickness can be approximated as:

$$h(\phi) = c \sin \phi \qquad (4.5)\ [1]$$

Where c is the feed rate (mm/tooth) and ϕ is the instantaneous angle of immersion. (This equation as well as the following equations comes from the same book [1].) Figure 4.2 shows the geometry of milling process.

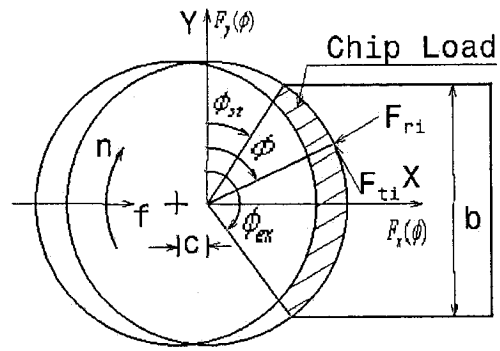

Figure 4.2 Geometry of Milling Process

If the helix angle of a cutter is zero, tangential ($F_t(\phi)$), radial ($F_r(\phi)$) and axial ($F_a(\phi)$) cutting forces can be expressed as:

$$\begin{cases} F_t(\phi) = K_{tc}ah(\phi) + K_{te}a \\ F_r(\phi) = K_{rc}ah(\phi) + K_{re}a \\ F_a(\phi) = K_{ac}ah(\phi) + K_{ae}a \end{cases} \tag{4.6}$$

Where $ah(\phi)$ is varying chip area, and a is edge contact length. K_{tc}, K_{rc} and K_{ac} are the cutting force coefficients in tangential, radial and axial directions, respectively. K_{te}, K_{re} and K_{ae} are the edge constants. The cutting coefficients are usually evaluated by milling tests or by using the following equations:

$$\begin{cases} K_{tc} = \dfrac{\tau_s}{\sin\phi_n} \dfrac{\cos(\beta_n - \alpha_n) + \tan i \cdot \tan\eta \cdot \sin\beta_n}{\sqrt{\cos^2(\phi_n + \beta_n - \alpha_n) + \tan^2\eta \cdot \sin^2\beta_n}} \\ K_{ac} = \dfrac{\tau_s}{\sin\phi_n \cdot \cos i} \dfrac{\sin(\beta_n - \alpha_n)}{\sqrt{\cos^2(\phi_n + \beta_n - \alpha_n) + \tan^2\eta \cdot \sin^2\beta_n}} \\ K_{rc} = \dfrac{\tau_s}{\sin\phi_n} \dfrac{\cos(\beta_n - \alpha_n) \cdot \tan i - \tan\eta \cdot \sin\beta_n}{\sqrt{\cos^2(\phi_n + \beta_n - \alpha_n) + \tan^2\eta \cdot \sin^2\beta_n}} \end{cases} \tag{4.7}$$

Where τ_s is the shear yield stress. β_n is the friction coefficient. i is the oblique angle. η is the chip flow angle. ϕ_n is the normal shear angle. α_n is the normal rake angle [10].

From Figure 4.2, it is simple to get feed, normal and axial components of the cutting forces. They are given by:

$$\begin{cases} F_x(\phi) = -F_t \cos\phi - F_r \sin\phi \\ F_y(\phi) = F_t \sin\phi - F_r \cos\phi \\ F_z(\phi) = +F_a \end{cases} \tag{4.8}$$

For a cutter with N teeth, the cutting forces are expressed as:

$$\begin{cases} F_x(\phi_j) = \sum_{j=1}^{N} F_{xj}(\phi_j) \\ F_y(\phi_j) = \sum_{j=1}^{N} F_{yj}(\phi_j) \\ F_z(\phi_j) = \sum_{j}^{N} F_{zj}(\phi_j) \end{cases} \tag{4.9}$$

When ϕ_j satisfies $\phi_{st} \le \phi_j \le \phi_{ex}$, Where ϕ_{ex} is the cutter exit angle, ϕ_{st} is the cutter entry angle. If the tooth j is out of the immersion zone, it contributes zero to total forces.

So the instantaneous resultant cutting force is given as:

$$F = \sqrt{F_x^2 + F_y^2 + F_z^2} \tag{4.10}$$

However, the situation changes when the helix angle is other than zero. This means that when the helix angle on a cutter is β, a point on the axis of the cutting edge will lag behind the end point of the tool [19]. Naturally, the lag factor will affect the performance

of the cutter so it must be taken into consideration [6]. The lag angle ψ at the axial depth of cut (z) is found as:

$$\tan\beta = \frac{D\psi}{2z} \quad \Rightarrow \psi = \frac{2z \cdot \tan\beta}{D} \tag{4.11}$$

Where D is the cutter diameter. Figure 4.3 shows the geometry of helical end milling.

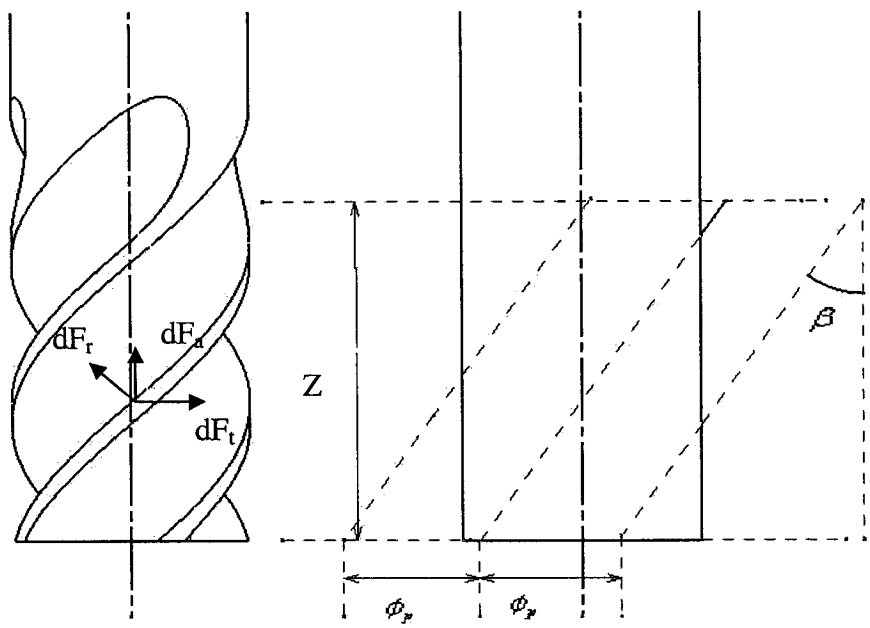

Figure 4.3 Geometry of Helical End Milling

It is worth a reminder that in the above steps, the cutting forces of the helix angle is taken as zero. If the angle is other than zero (as in real-life milling), further calculations are required. To carry out these calculations, the immersion angle for flute j at axial depth of cut z is:

$$\phi_j(z) = \phi + j\phi_p - k_\beta z \tag{4.12}$$

Where $\phi_p = \frac{2\pi}{N}$ is the tooth spacing angle. $k_\beta = (2\tan\beta)/D$.

Tangential ($dF_{t,j}$), radial ($dF_{r,j}$), and axial ($dF_{a,j}$) forces on a differential flute element are given by:

$$\begin{cases} dF_{t,j}(\phi,z) = [K_{tc}h_j(\phi_j(z)) + K_{te}]dz \\ dF_{r,j}(\phi,z) = [K_{rc}h_j(\phi_j(z)) + K_{re}]dz \\ dF_{a,j}(\phi,z) = [K_{ac}h_j(\phi_j(z)) + K_{ae}]dz \end{cases} \tag{4.13}$$

Where the chip thickness is $h_j(\phi_j(z) = c\sin(\phi_j(z))$. The feed (x), normal (y), and axial (z) cutting force are expressed as:

$$\begin{cases} dF_{x,j}(\phi_j,z) = -dF_{t,j}\cos\phi_j(z) - dF_{r,j}\sin\phi_j(z) \\ dF_{y,j}(\phi_j,z) = +dF_{t,j}\sin\phi_j(z) - dF_{r,j}\cos\phi_j(z) \\ dF_{z,j}(\phi_j,z) = +dF_{a,j} \end{cases} \tag{4.14}$$

Substituting the differential forces and the chip thickness into above equation will give the following result:

$$\begin{cases} dF_{x,j}(\phi_j,z) = \left\{ \begin{array}{l} \frac{c}{2}[-K_{tc}\sin 2\phi_j(z) - K_{rc}(1-\cos 2\phi_j(z))] \\ +[-K_{te}\cos\phi_j(z) - K_{re}\sin\phi_j(z)] \end{array} \right\} dz \\ dF_{y,j}(\phi_j,z) = \left\{ \begin{array}{l} \frac{c}{2}[K_{tc}(1-\cos 2\phi_j(z)) - K_{rc}\sin 2\phi_j(z)] + \\ [K_{te}\sin\phi_j(z) - K_{re}\cos\phi_j(z)] \end{array} \right\} dz \\ dF_{z,j}(\phi_j,z) = [K_{ac}c\sin\phi_j(z) + K_{ae}]dz \end{cases} \tag{4.15}$$

The differential cutting forces are integrated analytically along the in-cut portion of the flute j in order to obtain the total cutting force produced by the flute [20]:

$$F_q(\phi_j(z)) = \int_{z_{j.1}}^{z_{j.2}} dF_q(\phi_j(z))dz, q = x, y, z \tag{4.16}$$

Where $z_{j.1}(\phi_j(z))$ and $z_{j.2}(\phi_j(z))$ are the lower and upper axial engagement limits of the in-cut portion of the flute j. The integrations are carried out by: $\phi_j(z) = \phi + j\phi_p - k_\beta z$, $d\phi_j(z) = -k_\beta dz$. Thus

$$\begin{cases} F_{x,j}(\phi_j(z)) = \left\{ \begin{array}{l} \dfrac{c}{4k_\beta}[-K_{tc}\cos 2\phi_j(z) + K_{rc}(2\phi_j(z) - \sin 2\phi_j(z))] \\ + \dfrac{1}{k_\beta}[K_{te}\sin\phi_j(z) - K_{re}\cos\phi_j(z)] \end{array} \right\}_{z_{j.1}(\phi_j(z))}^{z_{j.2}(\phi_j(z))} \\ F_{y,j}(\phi_j(z)) = \left\{ \begin{array}{l} \dfrac{-c}{4k_\beta}[K_{tc}(2\phi_j(z) - \sin 2\phi_j(z)) + K_{rc}\cos 2\phi_j(z)] \\ + \dfrac{1}{k_\beta}[K_{te}\cos\phi_j(z) + K_{re}\sin\phi_j(z)] \end{array} \right\}_{z_{j.1}(\phi_j(z))}^{z_{j.2}(\phi_j(z))} \\ F_{z,j}(\phi_j, z) = \dfrac{1}{k_\beta}[K_{ac}c\cos\phi_j(z) - K_{ae}\phi_j(z)]_{z_{j.1}(\phi_j(z))}^{z_{j.2}(\phi_j(z))} \end{cases} \tag{4.17}$$

The cutting forces contributed by all flutes are calculated and summed to obtain the total instantaneous forces on the cutter at immersion ϕ:

$$\begin{cases} F_x(\phi) = \sum_{j=0}^{N-1} F_{xj} \\ F_y(\phi) = \sum_{j=0}^{N-1} F_{yj} \\ F_z(\phi) = \sum_{j=0}^{N-1} F_{zj} \end{cases} \tag{4.18}$$

The resultant cutting force acting on the milling cutter is

$$F(\phi) = \sqrt{F_x(\phi)^2 + F_y(\phi)^2 + F_z(\phi)^2} \tag{4.19}$$

The cutting force model can be efficiently implemented to the CAD/CAM systems for milling process simulation [1]. The mechanistic cutting force model can be used to estimate instantaneous cutting force magnitudes and directions. Therefore, it can be used to estimate tooth stresses, cutters shank stresses and cutting tool deflections [13]. The model has several parameters obtained from many experiments.

4.4 A New Method of Finding Maximum Cutting Force Based on the Fuzzy Logic System

When using the mechanistic cutting force model, it is very hard to get the exact maximum cutting force in different machines. The stiffness factor in each machine varies considerably and can cause tremendous differences. So a new approach is needed. This approach involves calculating the maximum cutting force based on the geometry features of a machined part using a fuzzy inference system.

In CNC profile milling, according to the two-dimension chip load model, the chip load of the cutter changes at different geometry shapes and the cutting force also changes. The changes in the chip load and the cutting force match the geometry variation along the part profile. The chip load at a cutter location is measured by the cutter engagement angle, and the cutter engagement angle can be calculated with the profile of the pre-machined part and the profile of the design part [10]. The engagement angle changes when the cutter is located at different points. For example, the cutter engagement angle is larger when the tool is in the concave shape than when it is in the convex shape. The larger the cutter engagement angle, the greater the cutting force; a common example of

this principle is the way that a household meat cleaver must be wielded with more force than a butcher's sharp blade. Finding the largest cutter engagement angle means finding the maximum cutting force. In CNC machining, the point on the machined part profile that has the largest cutter engagement angle must be the point which has the maximum cutting force.

The surface quality must be maintained at a constant level to avoid chatter, because if the surface quality is good at the point of the maximum cutting force, it will also be good at other points of the machined part.

Through real machining experiments, it is possible to determine the initial feed rate, which is the feed rate set at the point where the engagement angle is largest in order to get the maximum cutting force. It is a step-by-step process. First, by calculating the cutter engagement angle, the geometry point where the engagement angle is largest can be found. Then set a feed rate with a proper value to machine the part at this point. If there is no cutter wear or chatter, then increase the feed rate. If cutter wear or chatter happens, then decrease the feed rate. With several iterations, the initial feed rate can be found. Usually, the initial feed rate is very close to the feed rate given by an experienced operator. The initial feed rate is related with the workpiece material, cutter size and cutter material.

The next target is the main goal: the maximum cutting force. It can be found using the fuzzy cutting force model, which gets inputs from the initial feed rate and the radial and axial depth of cut. There are four steps to follow:

1) Find the largest engagement angle using an offset algorithm and a proposed algorithm to obtain the intersection point of two curves.

2) Locate the geometrical segment that has the largest engagement angle.

3) Find the initial feed rate experimentally, by checking the tool wear or chatter. If there is no tool wear or chatter, increase the feed rate. If there is tool wear or chatter, decrease the feed rate. Repeat as often as necessary.

4) After finding the initial feed rate, put the initial feed rate into the fuzzy cutting force model, and the maximum cutting force can be calculated.

Chapter 5 Procedure for Determination of Proper Feed Rate

5.1 Calculations for Cutter Engagement Angles

This section introduces the geometry that is used for calculating the cutter engagement angles. The section has two main parts: (1) offset algorithm for tool path generation; and (2) a proposed algorithm to obtain the intersection of two curves. Both parts are described in detail in the following.

5.1.1 Offset Algorithm for Tool Path Generation

For a CNC profile machining, the tool paths will be offset contour around a machining part. For example, in Figure 5.1, the part profile is the innermost shape and the contour of the machined part after rough machining is the middle shape. Based on the information about the design of the part and the cutter size, the tool path of the CNC profile milling is planned. It is the outermost shape. In this figure, the middle and outermost curves are the offset curves and the innermost curves denote the boundary of a machining part.

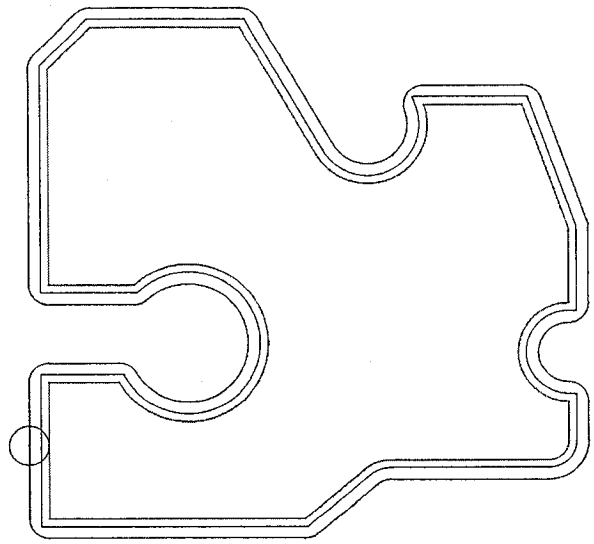

Figure 5.1 Tool Path of the Profile Milling

To obtain the tool paths of CNC profile milling and to calculate the engagement angles, it is very necessary to study the offset algorithms. The offset of a part boundary has been studied extensively. In CNC machining, three main algorithms are widely used: the pair-wise offset approach; the Voronoi diagram; and the pixel-based method. In this work, the pair-wise offset approach to calculate the profile tool path is adopted, because it is simple and intuitive. It is also widely used in industry practice even though it does have some drawbacks.

The Voronoi diagram method is more efficient and robust, but its weakness is numerical instability. The pixel-based approach overcomes the drawbacks of the pair-wise offset and the Voronoi diagram. However, this approach requires a huge amount of memory as well as too much computation time to achieve the desired level of precision [11].

For a program designed to do profile machining, the first step is to determine the shape of the part that is to be machined. The part's profile will usually include a combination of linear and circular segments, which are relatively simple to determine, as well as a sequence of curves that are approximated by the linear and circular segments.

The sequence curves in the part profile form a curve chain. As described by Hansen *et al* 1992 [16], the curve chain is defined as an ordered list of linear and circular curves. In mathematical terms, the definition of the curve chain is as follows: $\zeta = \{C_1, C_2, ...C_n\}$ where:

$$\begin{aligned} C_i &= C_i(t), \qquad 0 \le t \le 1, i = 1,2,...,n \\ C_i(1) &= C_{i+1}(0), \qquad i = 1,2,...,n-1 \end{aligned} \tag{5.1}$$

The points $C_i(0), i = 1,...,n$ and $C_n(1)$ are called the knot points of the curve chain, and $C_1(0)$ and $C_n(1)$ are called its end points [16].

The input of the offset algorithm consists of an offset distance (d) and a set of curved chains representing the peripheral boundary of a part, as shown in Figure 5.1. The output is a collection of curved chains and represents the offset of the peripheral boundary of the part. Usually, the offset distance d should be bigger than, or equal to, the tool radius.

Figure 5.2 shows a chain consisting of seven curves, of which two curves (C_4 and C_7) are circular.

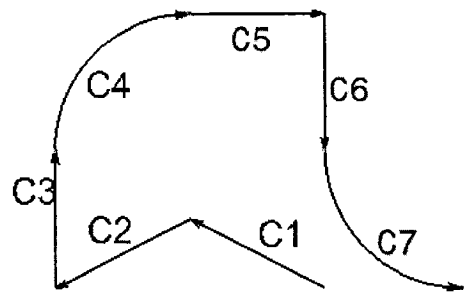

Figure 5.2 Chain of Curves

The algorithm of the pair-wise chain offset has two phases: (1) raw offset generation and (2) the raw offsets analysis. The first phase processes the input peripheral curved chains. When two first degree continuous segments are offset, the offset segments are connected and are first degree continuous, and the tangency condition is preserved. When two adjacent segments in an input chain are offset initially; to close the gap, it is necessary to insert an extra circular arc in the offset chain (see Figure 5.3). The inserted arc represents the tool rolling around the common vertex of the two segments. At convex corners, the inserted arc may become a part of the output tool path, if it does not cause interference elsewhere.

The second phase of the algorithm involves the detection of all pair-wise self-intersections in the raw offset-curve, and the removal of all invalid loops. The details about the raw offsets analysis can be found in [11]. Because many CAD/CAM software packages already provide the functions of the phase, in this work, the functions of the phase provided by CATIA are used to analyse the raw offsets.

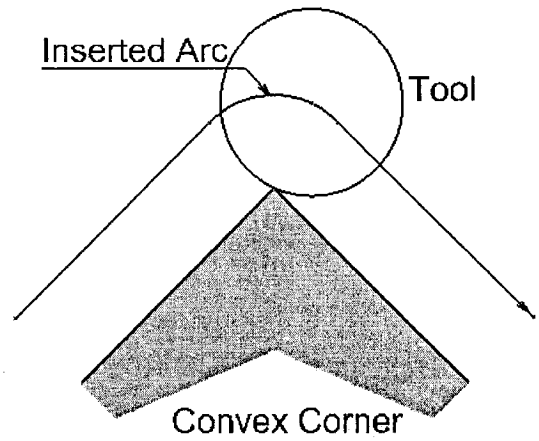

Figure 5.3 Convex Corner and Inserted Arc

Based on the pair-wise offset algorithm, the offset part profile for the tool path is generated in this work. The application of the offset part profile can be seen in Figure 5.1, where the middle and outermost shapes are the offset curves.

5.1.2 Engagement Angle

After the offset tool paths are obtained, the next step is to find the exact intersection points of the cutter and the semi-finished part edges. In Figure 5.1, the intersection points as shown are between the small circle which represents the cutter, and the middle curve chain, which represents the semi-finished part edge. The simplest and most common method to determine the intersection points involves the use of a mathematical formula which will be explained later [30].

The question of finding an intersection point is a fundamental construct in many computer graphics and modeling applications. Usually, for computing intersections of lines and segments in 2D, it is best to use an equation representation [29]. The

algorithms for the simplest 2D linear primitives and linear segments will be examined in detail.

Figure 5.4 shows the engagement angle. The intersection point between the cutter and work piece is calculated using the cutter geometry equation and the geometry equation of a previously machined work piece. The engagement angle can be easily obtained from calculated intersection point [29].

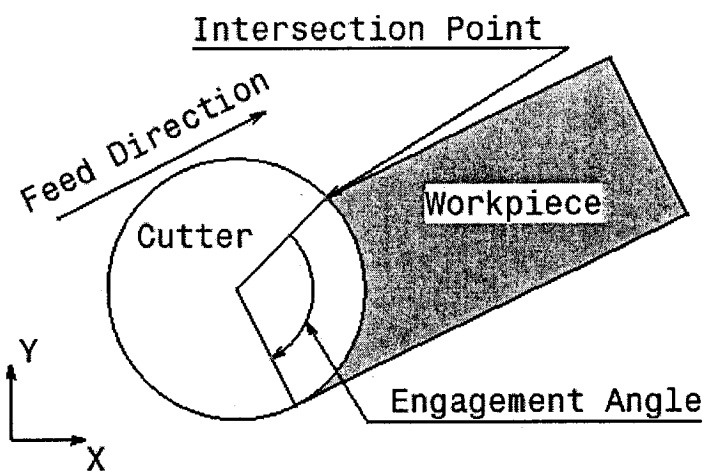

Figure 5.4 Intersection Point

The cutter movement is composed of line and circular segments. The boundary of the machined workpiece remains as a combination of line and arc segments. Figure 5.5 (a) and (b) shows the boundary of workpiece generated by cutter movement along line path and arc path, respectively. The line and arc segment to present the boundary of machined workpiece have information such as start point, (x_{ws}, y_{ws}), end point, (x_{we}, y_{we}), slope angle, α_l, start angle of arc, α_s, end angle of arc, α_e, center of arc, (w_{cx}, w_{cy}) and radius of arc, w_r.

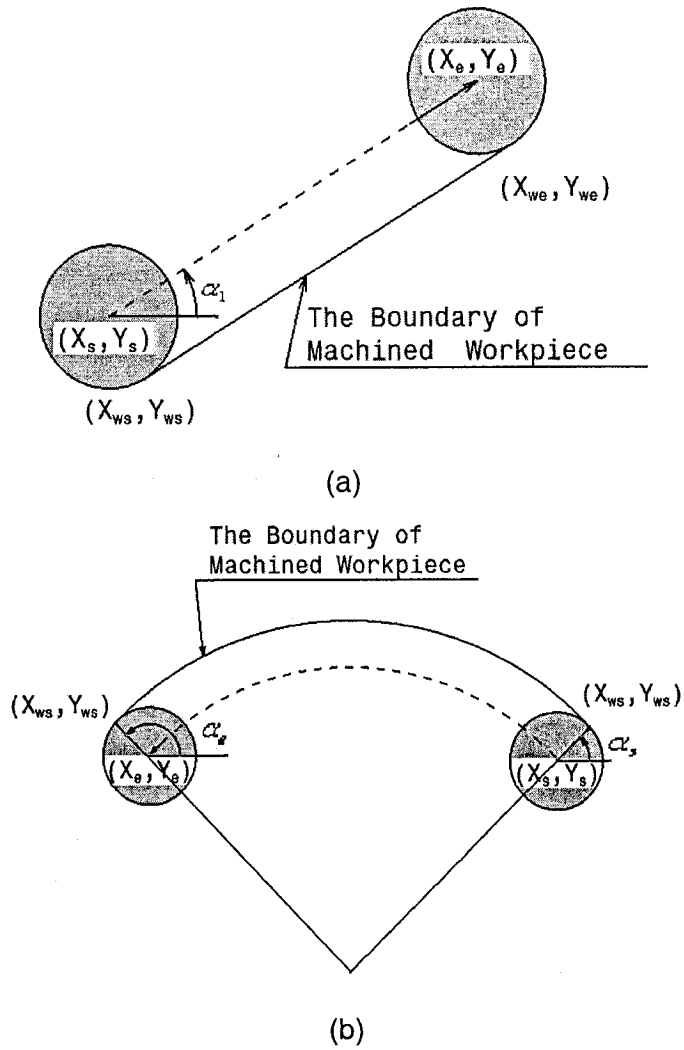

Figure 5.5 Intersection Point Calculation (a) When a Cutter Movement along Line Paths (b) When a Cutter Movement along Arc Paths

The procedure to calculate intersection point between the line segment of the workpiece boundary and circle geometry of cutter is as follows.

The cutter geometry and the boundary geometry of pre-machining workpiece can be defined as Equations 5.2 and 5.3.

$$(x-t_{cx})^2+(y-t_{cy})^2=t_r^{\ 2} \tag{5.2}$$

where (t_{cx}, t_{cy}) is the current position of tool and t_r is the radius of tool.

$$y = ax + b \tag{5.3}$$

where $a = \frac{(y_{we} - y_{ws})}{(x_{we} - x_{ws})}$ and $b = y_{ws} - ax_{ws}$. x value of intersection point can be calculated using Equation 5.4.

$$x_t = \frac{-B \pm \sqrt{(B^2 - 4AC)}}{2A} \tag{5.4}$$

where $A = 1 + a^2$, $B = 2a(b - t_{cy}) - 2t_{cx}$ and $C = (b - t_{cy})^2 - t_r^{\ 2} + t_{cx}^{\ 2}$.

If x_{we} equals to x_{ws}, x value of intersection point is as follows:

$$x_t = x_{we} \tag{5.5}$$

y value of intersection point can be derived from Equations 5.5 and 5.6.

$$y_t = t_{cy} \pm \sqrt{(t_r^{\ 2} - (x_{we} - t_x)^2)} \tag{5.6}$$

where (x_t, y_t) is intersection point of tool and workpiece.

The following equations show the procedure to calculate intersection point between the arc segment of the workpiece boundary and the circle geometry of tool. Tool geometry equation is the same as Equation 5.2. The equation of the arc segment of pre-machining workpiece is defined as follows:

$$(x - w_{cx})^2 + (y - w_{cy})^2 = w_r^2 \tag{5.7}$$

When Equation 5.2 minus Equation 5.7, the following equation can be obtained:

$$x = -Py + Q \tag{5.8}$$

where $P = \dfrac{t_{cy} - w_{cy}}{t_{cx} - w_{cx}}$ and $Q = \dfrac{w_r^{\ 2} - t_r^2 + t_{cx}^2 + t_{cy}^2 - w_{cx}^2 - w_{cy}^2}{2(t_{cx} - w_{cx})}$. The intersection point can be derived from Equations 5.9 and 5.10.

$$y_t = \frac{-B \pm \sqrt{(B^2 - 4AC)}}{2A} \tag{5.9}$$

$$x_t = -Py_t + Q \tag{5.10}$$

where $A = 1 + P^2$, $B = -(2PQ - 2t_{cx}P + 2t_{cy})$ and $C = Q^2 + t_{cx}^2 - 2t_{cx}Q + t_{cy}^2 - t_t^2$.

If t_{cx} equals to w_{cx}, intersection point can be derived follows.

$$y_t = a \tag{5.11}$$

$$x_t = t_{cx} \pm \sqrt{t_r^2 - (a - t_{cy})^2} \tag{5.12}$$

where $a = \dfrac{(-w_r^2 + t_r^2 - t_{cy}^2 + w_{cy}^2)}{2(w_{cy} - t_{cy})}$

Thus the engagement angle can be accurately calculated following the movement of tool by using the intersection points of the cutter and the workpiece. The algorithm used in this paper to calculate the intersect point is a simple one but it's not such an easy matter to determine the program code for the intersection of two segments. Many special cases need to be checked (see the programming code).

Based on this algorithmic method, the intersect points between the pre-machining part edges (the middle curves in Figure 5.1) and the cutter (the small circle in Figure 5.1) can be computed efficiently. Therefore, the engagement angle of each point can be obtained.

5.2 Final Calculations for Proper Feed Rate

Once the fuzzy cutting force model has been established, and the engagement angle of each point is obtained, final calculations can be done for the proper feed rate. For these calculations, the inputs are: (1) the axial depth of cut; (2) the radial depth of cut, which is computed by the engagement angles of each part point; (3) the initial feed rate, which is obtained by experiment; and (4) the maximum cutting force, which is obtained by the approach based on geometry features. The maximum cutting force provides a reference for the proper feed rate.

By using the fuzzy system, the cutting force can be estimated when the depth of cut and the feed rate are known. It will be recalled that the maximum cutting force will be higher as the feed rate decreases, and lower as the feed rate increases. To reach the main objective - finding the proper feed rate - there are five steps to follow:

1) Set the axial depth of cut for each profile machining. Locate the geometry features of the part profile. Calculate the cutter engagement angles and the radial depth of cut for each geometry feature. Find an initial feed rate.

2) Using the approach based on the geometry feature, find the maximum cutting force based on the work piece material, cutter size and cutter material.

3) Apply the fuzzy system to find the cutting force for each geometry feature.

4) Compare the cutting force with the maximum cutting force; if the cutting force is less than the maximum cutting force, increase the feed rate; if the cutting force is greater than the maximum cutting force, decrease the feed rate. Repeat Step 3 for each geometry feature until a setting close to the maximum cutting force is obtained.

5) After finding the proper feed rate for one feature, move to the next feature, and return to Steps 3 and 4. Once the proper feed rate has been found for all features, end the program.

Chapter 6 Applications and Programming of a Feed Rate Determination System

6.1 Applications

The approach described in this thesis offers major advantages in planning the feed rate for CNC profile machining. For example, consider a piece of stock material that is 130 *mm* long, 125 *mm* wide and 20 *mm* deep. In Figure 6.1, such a piece of stock material is shown as transparent and mounted on a platform. A flat end mill with the radial of 10 *mm* is used to machine the part, with the axial depth of cut set as 5 *mm*.

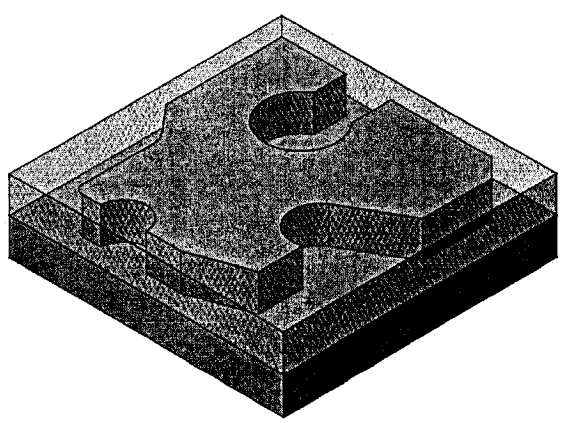

Figure 6.1 Example Part on a Platform and a Stock

In Figure 6.2, the flat end mill is shown. The overall length, the cutting length, and the body diameter of the cutter are 100 *mm*, 50 *mm*, and 15 *mm*, respectively. The cutter has two flutes, and its rake angle is 0 degrees. The tooth material is high speed steel.

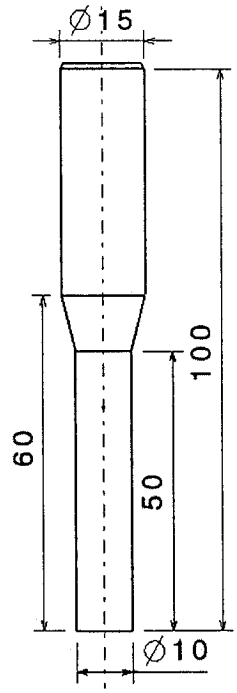

Figure 6.2 Flat End Mill

In this example, there are two machining stages. The first step is rough machining, which aims to remove material as quickly as possible. Therefore, the surface quantity is not the most important thing. In this stage, the parameters of rough machining were chosen by an experienced CNC operator. The approach feed rate was 300 *mm/min*, the machining feed rate was 220 *mm/min*, and the retract feed rate was 1000 *mm/min*. In Figure 6.3, the innermost shape, which combines arcs and straight lines, indicates the designed part edge, and the black circle is the cutter. The tool paths for the rough machining are the other lines. The material that remains after rough machining is

handled by finishing machining. The setting for finishing machining is 2*mm* offset from the designed part.

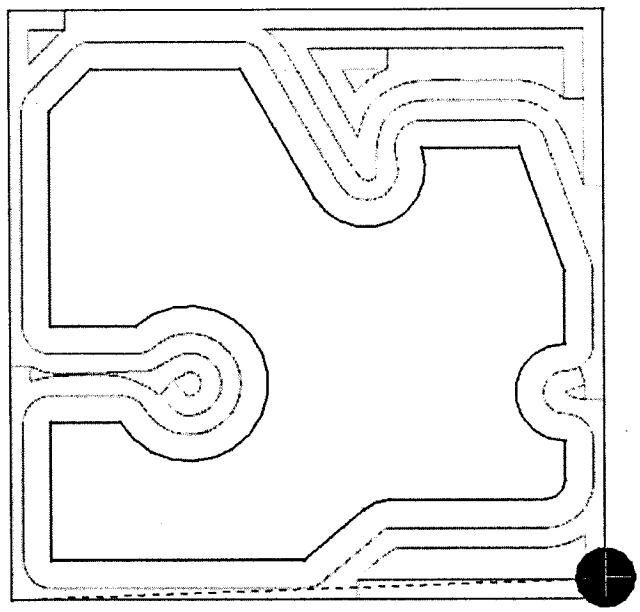

Figure 6.3 Rough Mill Tool Paths

In finishing machining, the feed rate is determined using the fuzzy logic cutting force model. Firstly, profile tool paths should be generated using the offset algorithm. The process is shown in a previous illustration, Figure 5.1, where the part profile is the innermost line and the machined part after rough machining is the middle line. The tool path of CNC profile milling, which is the outermost line, is based on information about the design of the part and the cutter size.

By evaluating the part profile, the convex turn, concave turn, and concave arcs with different radius are located. For each geometry feature, the cutter engagement angle is calculated, using the curves intersect method previously discussed. The cutter engagement angles are shown in Figure 6.4. It can be seen that at the C-D, I-J, M-N, and R-Q segments, the cutter engagement angles have a relatively high value. The cutter

engagement angles are listed in Table 6.1. It will be noted that the angles at the turning points vary considerably, ranging from a low of 40.56° at the O-P segment corner to a high of 73.74° at the R-Q segment corner. Elsewhere, cutter engagement angles have a uniform value of 53.13° at such segments as B-C, F-G, H-I, etc. The engagement angle data is vital for determining the proper feed rates for each geometry feature in part-profile machining. The proper feed rates for each geometry feature are listed in Table 6.1.

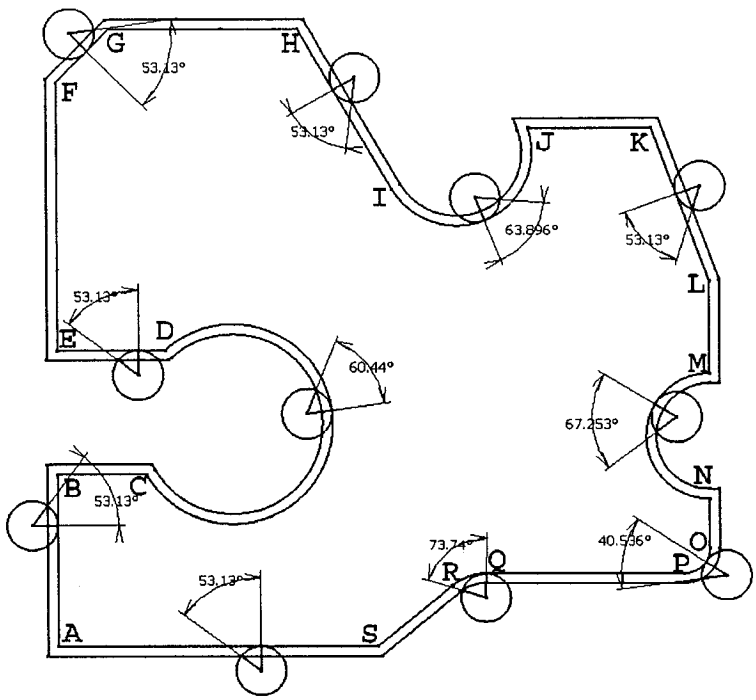

Figure 6.4 Engagement Angles

Table 6.1 Feed Rates for Different Geometric Features

	Tool Path Segments					
	A-B	C-D	I-J	M-N	O-P	R-Q
Engagement Angle (Degree)	53.13	60.44	63.89	67.25	40.56	73.74
Feed Rate (*mm/min*)	163	156	150	143	180	135

6.2 Numerical Control Code Optimization

Now that the proper feed rate has been determined for each segment of a profile CNC tool path, it's time for the final step. This involves the introduction of NC code optimization.

6.2.1 APT (Automatic Programmed Tools)

Several NC computer languages have been developed over the years, but there is still a lot of merit in the earliest one, APT (Automatic Programmed Tools). It can simultaneously generate complex geometry in all five of the machine's axes, and can do all types of programming. It also can generate the CNC tool path. For these reasons, APT is still in use in some aerospace companies, and most CAD/CAM software has the interface of APT. The postprocessor engine used by many of today's CAD/CAM and solid modeling systems is APT-based. With a basic understanding of APT, it is possible to do NC codes optimization [15] [30].

An APT program is comprised of a geometry section and a motion section. In the geometry section, the programmer defines the shape of the part, using APT language. In the motion section, the programmer describes the tool motion used to produce the part. This includes such instructions as controlling a spindle, defining feed rate and spindle speed, turning on a coolant, etc.

In the geometry section of an APT program, all geometry statements are constructed in the same logical manner:

<Geometry Name> = MAJOR WORD/<definition> [30]

The <Geometry Name> is any name, up to 6 characters, that the programmer assigns to the definition. Generally, the programmer assigns names in the following manner: P1, P2, P3, etc., for points; L1, L2, etc., for lines; C1, C2, etc., for circles; PL1, PL2, etc., for planes; and so on. MAJOR WORD is the geometry type defined (POINT, LINE, CIRCLE, PLANE). The <definition> is the statement or statements that match the geometry.

Here are some geometry examples: P1 =POINT/6, 6, 6 (Point defined by its Cartesian coordinates.); P2 =POINT/INTOF, L1, L2 (Intersection of lines L1 and L2.); P3 =POINT/CENTER, C1 (Center of circle C1.), etc.

All APT motion statements are constructed as follows:

MAJOR WORD/minor word

The MAJOR WORD is the command word, such as SPINDL, GOTO, CYCLE, and so on. The minor word is a descriptor word, such as IPM (inch per minute), IPR (inch per revolution), RPM (revolutions per minute), ON, OFF, and so on. Not all APT motion statements have minor words.

The following sequence is an example of APT motion statements.

FROM/0, 0, 0

SPINDL/RPM, 2500, CLW

FEDRAT/20, IPM

RAPID

GO/TO, L1

GOFWD/C1, TANTO, L2

GOTO/0, 0, 0

Once the structure of APT language has been understood, the next step is to modify the APT file to optimize the NC code. The proper feed rates, found in Table 6.1, are entered in the APT file, and the APT file is then put into a post processor. The processor's output is the crucial answer: the optimized NC code. Examples of APT codes, first without and then with optimized feed rates, are shown in Figures 6.5 and 6.6, respectively.

```
PPRINT OPERATION NAME : Profile Contouring.1
$$ Start generation of : Profile Contouring.1
LOADTL/1,1
FEDRAT/ 1000.0000,MMPM
SPINDL/   70.0000,RPM,CLW
GOTO/   73.90000,    4.80000,   35.20000
GOTO/   10.00000,    4.80000,   35.20000
AUTOPS
INDIRV/   -1.00000,    0.00000,    0.00000
TLON,GOFWD/(CIRCLE/     10.00000,     10.00000,     35.20000,$
      5.20000),ON,(LINE/     10.00000,     10.00000,     35.20000,$
   4.80000,     10.00000,     35.20000)
GOTO/    4.80000,   45.00000,   35.20000
AUTOPS
INDIRV/    0.00000,    1.00000,    0.00000
TLON,GOFWD/(CIRCLE/     10.00000,     45.00000,     35.20000,$
      5.20000),ON,(LINE/     10.00000,     45.00000,     35.20000,$
  10.00000,     50.20000,     35.20000)
GOTO/   27.68000,   50.20000,   35.20000
AUTOPS
INDIRV/    1.00000,    0.00000,    0.00000
TLON,GOFWD/(CIRCLE/     27.68000,     45.00000,     35.20000,$
      5.20000),ON,(LINE/     27.68000,     45.00000,     35.20000,$
  32.18330,     47.60006,     35.20000)
AUTOPS
INDIRV/    0.50001,   -0.86602,    0.00000
TLON,GOFWD/(CIRCLE/     45.00000,     55.00000,     35.20000,$
     14.79956),ON,(LINE/     45.00000,     55.00000,     35.20000,$
  59.52416,     52.15823,     35.20000)
AUTOPS
INDIRV/    0.19202,    0.98139,    0.00000
TLON,GOFWD/(CIRCLE/     45.00000,     55.00000,     35.20000,$
     14.79956),ON,(LINE/     45.00000,     55.00000,     35.20000,$
  35.02972,     65.93712,     35.20000)
AUTOPS
INDIRV/   -0.73902,   -0.67369,    0.00000
TLON,GOFWD/(CIRCLE/     31.52654,     69.78000,     35.20000,$
      5.20000),ON,(LINE/     31.52654,     69.78000,     35.20000,$
```

Figure 6.5 Examples of APT Codes without Proper Feed Rate

```
PPRINT OPERATION NAME : Profile Contouring.1
$$ Start generation of : Profile Contouring.1
LOADTL/1,1
FEDRAT/ 1000.0000,MMPM
SPINDL/   70.0000,RPM,CLW
GOTO/   73.90000,    4.80000,   35.20000
GOTO/   10.00000,    4.80000,   35.20000
AUTOPS
INDIRV/   -1.00000,    0.00000,    0.00000
TLON,GOFWD/(CIRCLE/     10.00000,     10.00000,     35.20000,$
      5.20000),ON,(LINE/     10.00000,     10.00000,     35.20000,$
   4.80000,     10.00000,     35.20000)
FEDRAT/ 163.0000,MMPM
GOTO/    4.80000,   45.00000,   35.20000
AUTOPS
INDIRV/    0.00000,    1.00000,    0.00000
TLON,GOFWD/(CIRCLE/     10.00000,     45.00000,     35.20000,$
      5.20000),ON,(LINE/     10.00000,     45.00000,     35.20000,$
  10.00000,     50.20000,     35.20000)
GOTO/   27.68000,   50.20000,   35.20000
AUTOPS
INDIRV/    1.00000,    0.00000,    0.00000
FEDRAT/ 156.0000,MMPM
TLON,GOFWD/(CIRCLE/     27.68000,     45.00000,     35.20000,$
      5.20000),ON,(LINE/     27.68000,     45.00000,     35.20000,$
  32.18330,     47.60006,     35.20000)
AUTOPS
INDIRV/    0.50001,   -0.86602,    0.00000
TLON,GOFWD/(CIRCLE/     45.00000,     55.00000,     35.20000,$
     14.79956),ON,(LINE/     45.00000,     55.00000,     35.20000,$
  59.52416,     52.15823,     35.20000)
AUTOPS
INDIRV/    0.19202,    0.98139,    0.00000
TLON,GOFWD/(CIRCLE/     45.00000,     55.00000,     35.20000,$
     14.79956),ON,(LINE/     45.00000,     55.00000,     35.20000,$
  35.02972,     65.93712,     35.20000)
FEDRAT/ 150.0000,MMPM
AUTOPS
INDIRV/   -0.73902,   -0.67369,    0.00000
```

Figure 6.6 Examples of APT Codes with Proper Feed Rate

Using the feed rates determined with this proposed method, the total machining time of a profile milling part would be 39 minutes and 34 seconds, using an unmanned machine without any tool breakage or impaired surface quality. By comparison, a machine run by an experienced operator with a feed rate that consistently averages 135 *mm/min* would take 48 minutes and 36 seconds to machine

the same part. This means the proposed approach would reduce machining time by 18.6%.

The profile machining of the part, with the proper feed rates in CATIA CAD/CAM system, is depicted in Figure 6.7. Examples of NC codes, without optimized feed rate and then with optimized feed rate, are shown in Figures 6.8 and 6.9, respectively.

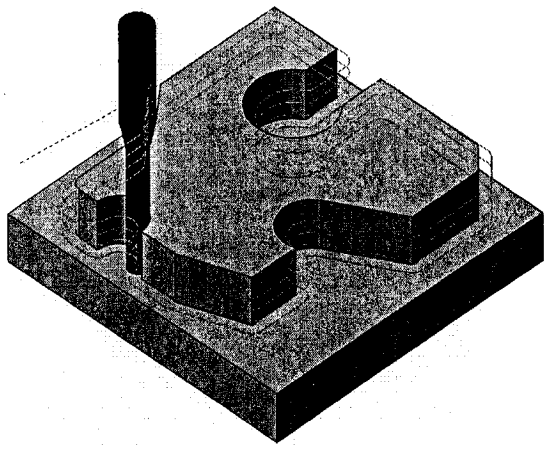

Figure 6.7 Simulation of Profile Finishing Machining

```
N15 F300.
N20 G40 G0 X6.181 Y.221 S+
N25 G0 Z1.772
N30 G1 Z1.378
N35 G1 X5.906
N40 F135.
N45 G1 Y.028
N50 G1 X5.9 Y+0
N55 G1 X3.424
N60 G1 Y.197
N65 G1 X3.426 Y.199
N70 G1 X3.59 Y.355
N75 G1 X3.772 Y.488
N80 G1 X3.816 Y.512
N85 G1 X5.31
N90 G1 X5.341 Y.514
N95 G1 X5.471 Y.546
N100 G1 X5.595 Y.597
N105 G1 X5.709 Y.667
N110 G1 Y.415
N115 G1 Y.197
N120 G1 X3.424
N125 G1 Y+0
N130 G1 X.028
N135 G1 X+0 Y.028
N140 G1 Y2.335
N145 G1 X.197
N150 G1 X.281 Y2.298
N155 G1 X.371 Y2.278
N160 G1 X.589 Y2.26
N165 G1 X.808 Y2.262
N170 G1 X1.026 Y2.283
N175 G1 X1.156 Y2.293
N180 G1 X1.286 Y2.285
N185 G1 X1.342 Y2.286
N190 G1 X1.395 Y2.303
N195 G1 X1.523 Y2.368
N200 G1 X1.647 Y2.442
N205 G1 X1.701 Y2.467
N210 G1 X1.759 Y2.478
N215 G1 X1.85 Y2.47
N220 G1 X1.934 Y2.435
N225 G1 X2.005 Y2.377
N230 G1 X2.056 Y2.301
N235 G1 X2.082 Y2.214
N240 G1 Y2.123
```

Figure 6.8 Examples of NC Codes without Proper Feed Rate

```
N15 F300.
N20 G40 G0 X6.181 Y.221 S+70
N25 G0 Z1.772
N30 G1 Z1.378
N35 G1 X5.906
N40 F135.
N45 G1 Y.028
N50 G1 X5.9 Y+0
N55 G1 X3.424
N60 G1 Y.197
N65 G1 X3.426 Y.199
N70 G1 X3.59 Y.355
N75 G1 X3.772 Y.488
N80 G1 X3.816 Y.512
N85 G1 X5.31 F163.
N90 G1 X5.341 Y.514
N95 G1 X5.471 Y.546
N100 G1 X5.595 Y.597
N105 G1 X5.709 Y.667
N110 G1 Y.415 F156.
N115 G1 Y.197
N120 G1 X3.424
N125 G1 Y+0
N130 G1 X.028
N135 G1 X+0 Y.028
N140 G1 Y2.335
N145 G1 X.197 F150.
N150 G1 X.281 Y2.298
N155 G1 X.371 Y2.278
N160 G1 X.589 Y2.26
N165 G1 X.808 Y2.262
N170 G1 X1.026 Y2.283
N175 G1 X1.156 Y2.293
N180 G1 X1.286 Y2.285
N185 G1 X1.342 Y2.286
N190 G1 X1.395 Y2.303
N195 G1 X1.523 Y2.368
N200 G1 X1.647 Y2.442
N205 G1 X1.701 Y2.467
N210 G1 X1.759 Y2.478
N215 G1 X1.85 Y2.47
N220 G1 X1.934 Y2.435
N225 G1 X2.005 Y2.377
N230 G1 X2.056 Y2.301
N235 G1 X2.082 Y2.214
N240 G1 Y2.123
```

Figure 6.9 Examples of NC Codes with Proper Feed Rate

6.3 Proper Feed Rate Determination Programming System

In this work, many technologies and algorithms have been used to determinate the proper feed rates. To make the method easy to apply, the generic and intelligent feed rate

determination programming system was established. Figure 6.10 shows the starting window of the system.

Figure 6.10 Starting Window

The main interface of the system is shown in Figure 6.11.

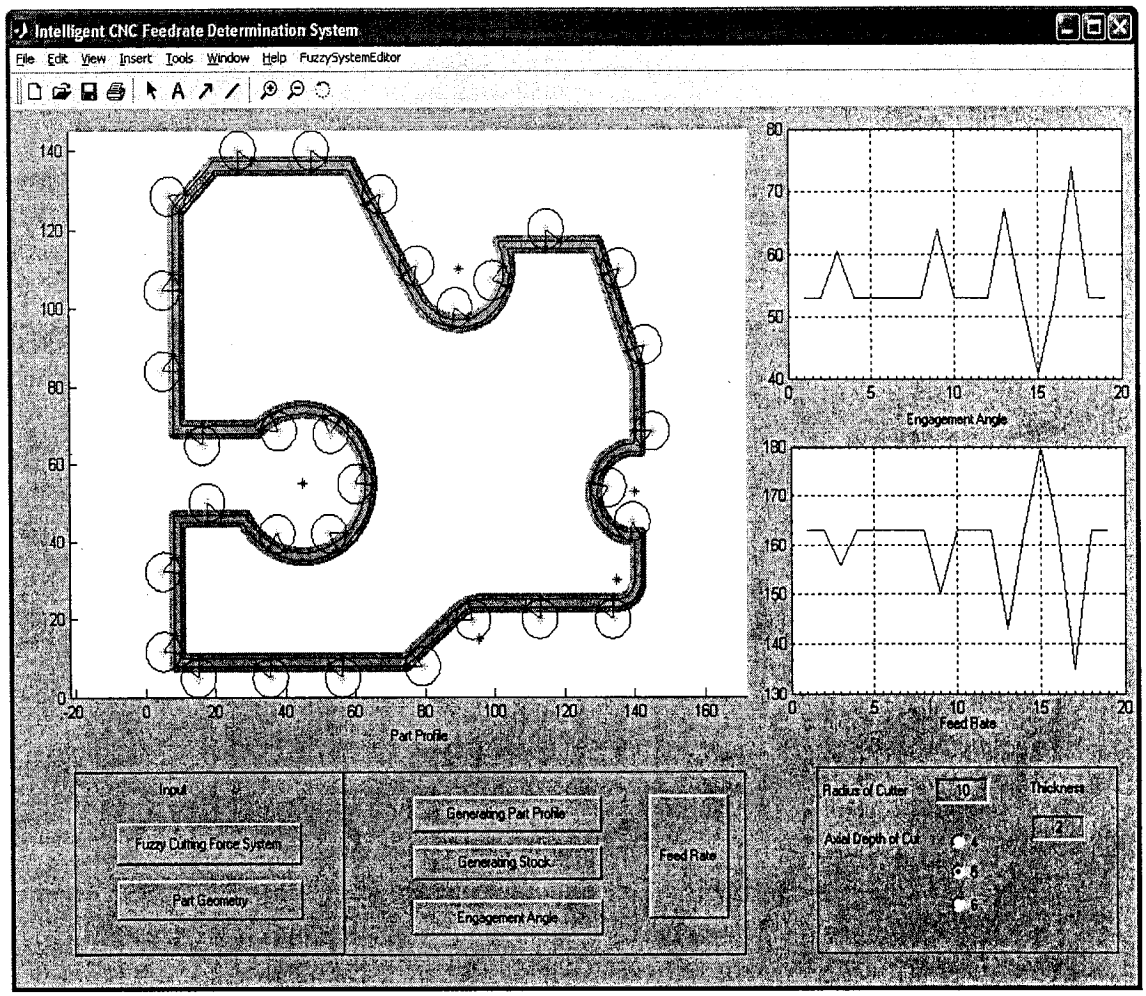

Figure 6.11 Main Window of Generic and Intelligent Feed Rate Determination System

As can be seen, there are two input commands: fuzzy cutting force system, and part geometry. There are four output commands: generating part profile; generating stock, (which is based on the right thickness value); engagement angle; and feed rate. The system has several main functions, including part geometry which allows for the initial inputting of part geometry data. This function has the following interface:

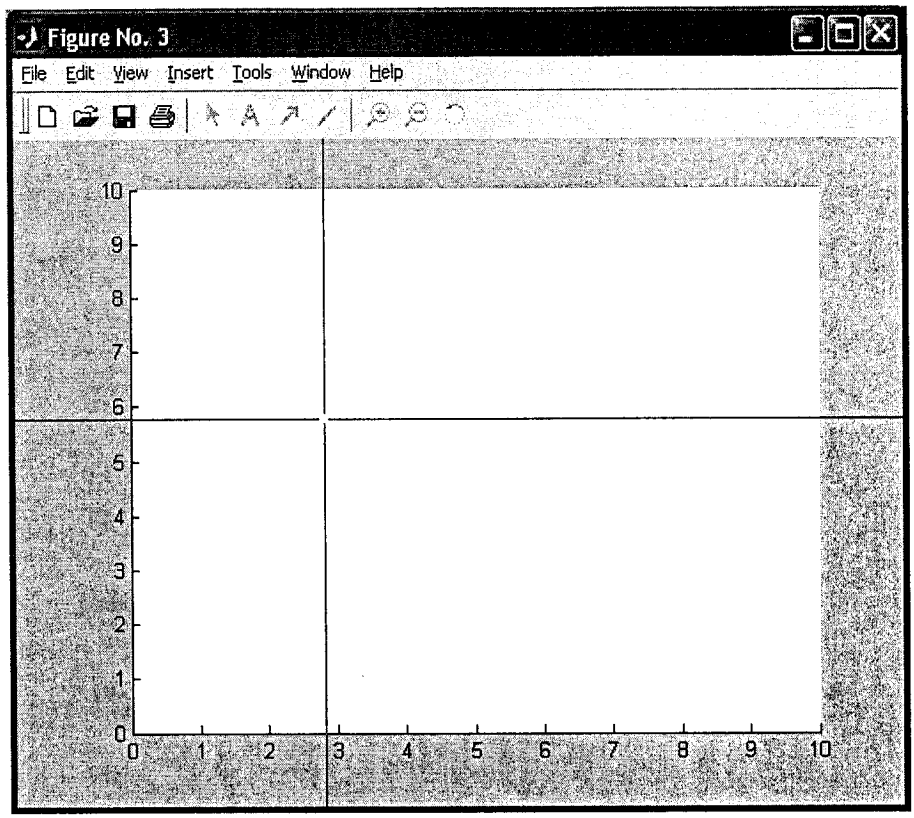

Figure 6.12 Window of Drawing Part Geometry

The second function is the fuzzy logic cutting force inference system. Figure 6.13 shows an overview diagram of a cutting force fuzzy system. Inputs and their membership functions appear to the left of the fuzzy cutting force system structural characteristics, while outputs and their membership functions appear on the right.

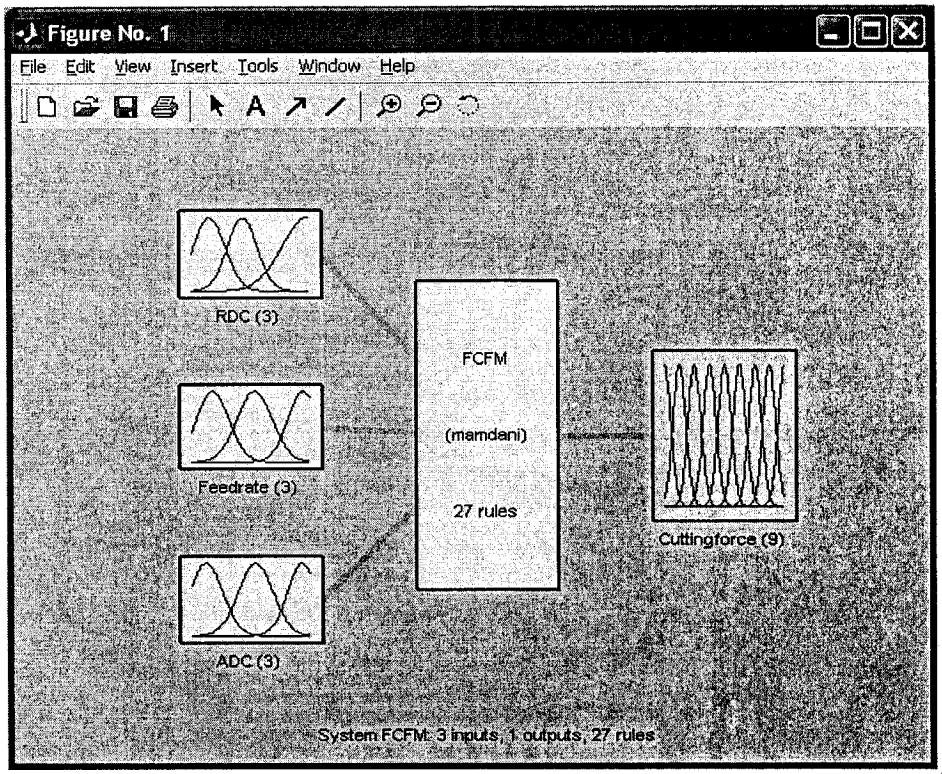

Figure 6.13 Window of Fuzzy System Structure

The third function, the fuzzy system editor, is in the menu of fuzzy system editor (see Figure 6.14). This menu has three sub-functions: (1) the fuzzy inference system (FIS), which can edit the structure of a fuzzy system (see Figure 6.15); (2) the fuzzy function, which is the editor of a fuzzy membership function (see Figure 6.16); (3) the surface function, which can show the surface of a fuzzy system (see Figure 6.17).

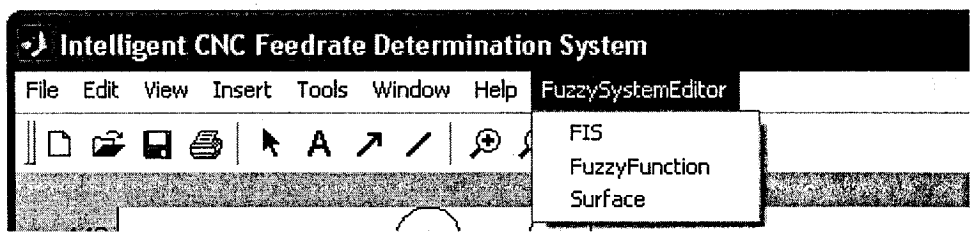

Figure 6.14 Menu of Fuzzy System Editor

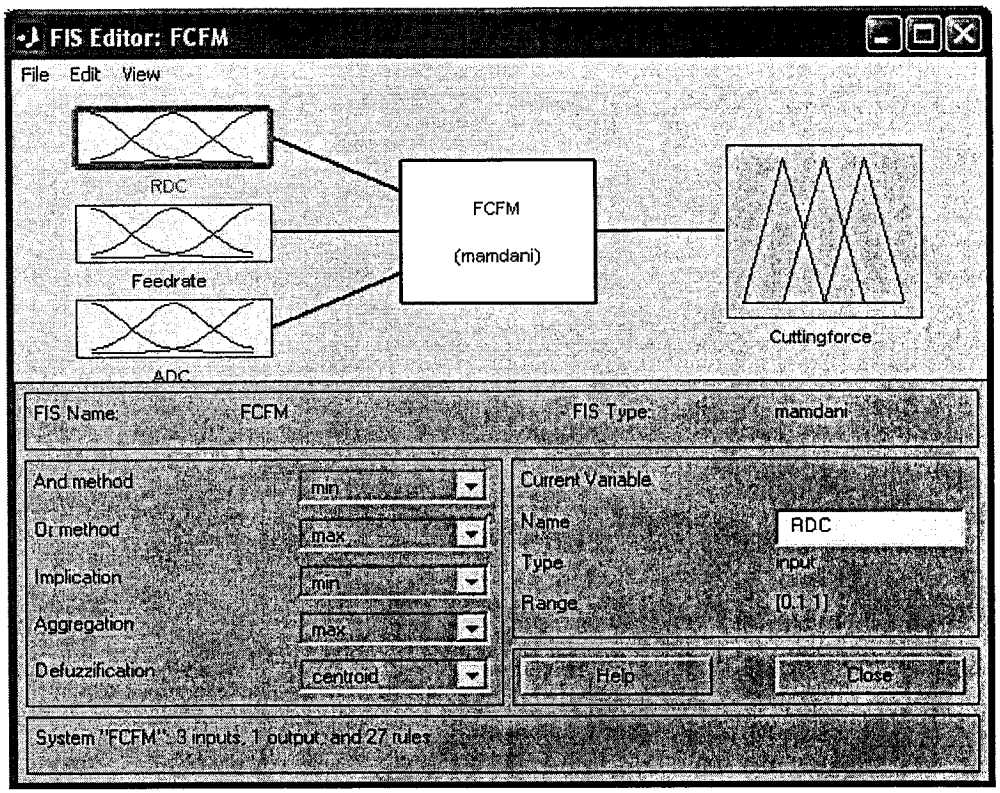

Figure 6.15 Window of FIS Editor

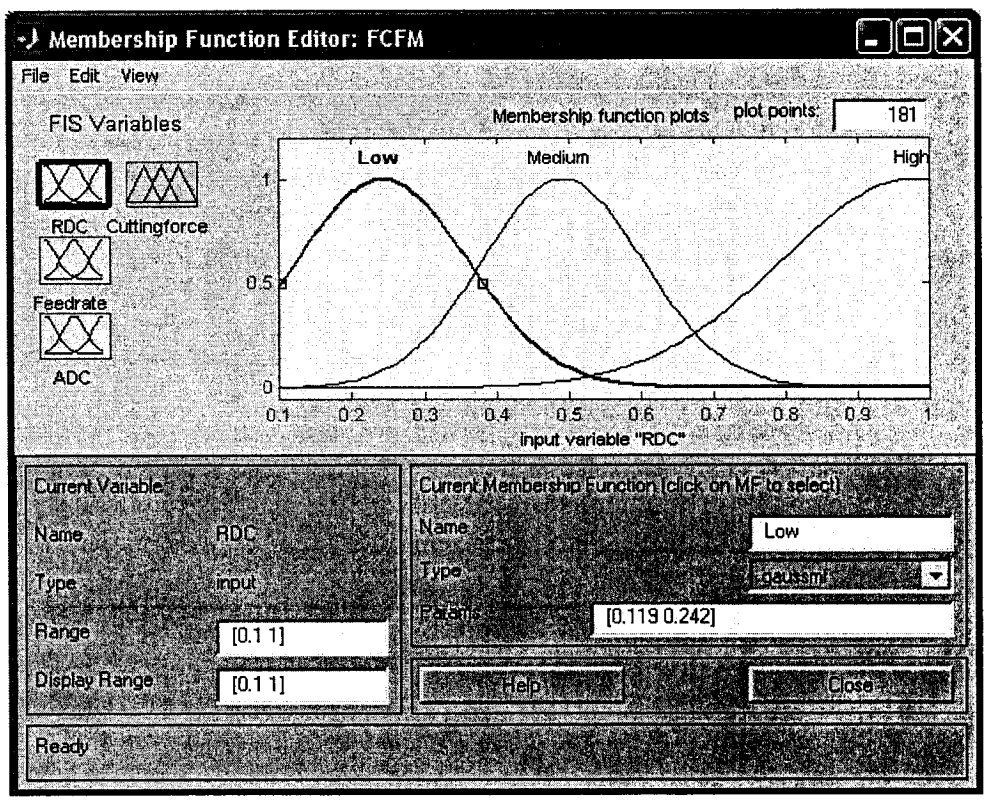

Figure 6.16 Window of Membership Function Editor

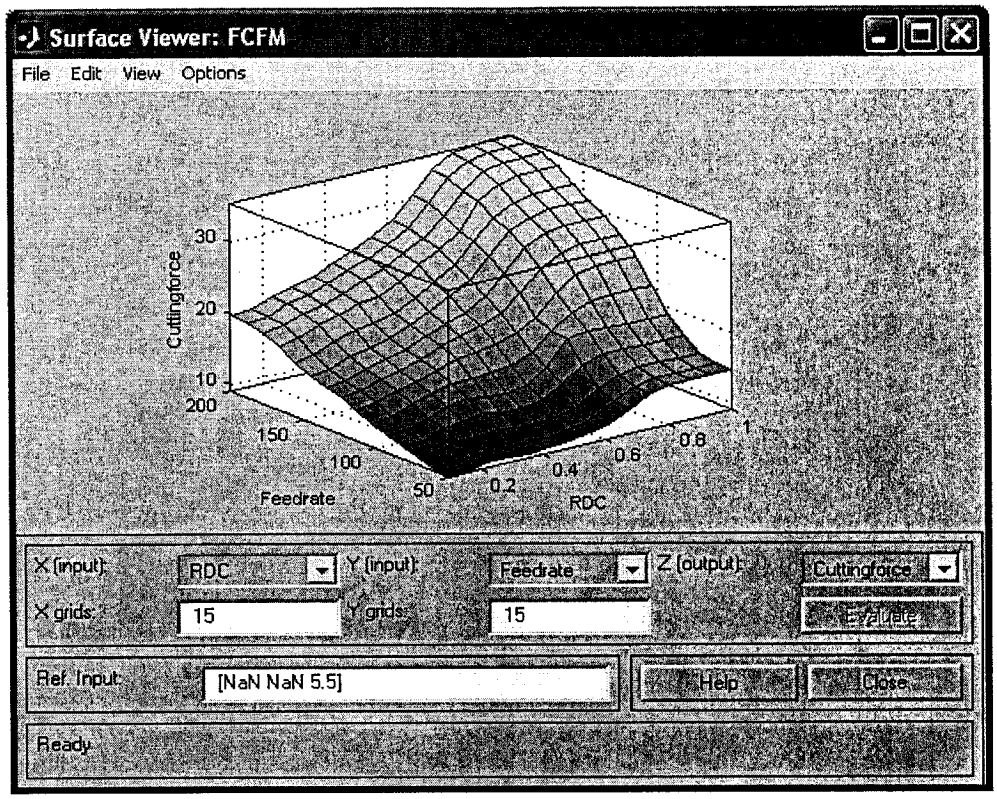

Figure 6.17 Window of Surface Viewer

6.4 Verification with Machined Parts

In this work, two identical parts are machined to demonstrate the greater efficiency of the proper feed rate determination. Two layers are machined in one part, and four layers are machined in the other part. The generic and intelligent approach is applied on a part that is designed on CATIA v5 CAD/CAM system. The part is shown in Figure 6.1. A DECKEL MAHO CNC milling machine is used to machine the part (see Figure 6.18). The material of the part is aluminium (6061 T6). A high-speed-steel flat end-mill with a 0.375 *inch* diameter is used for the part's rough and finish machining. The machined part is shown in Figure 6.19.

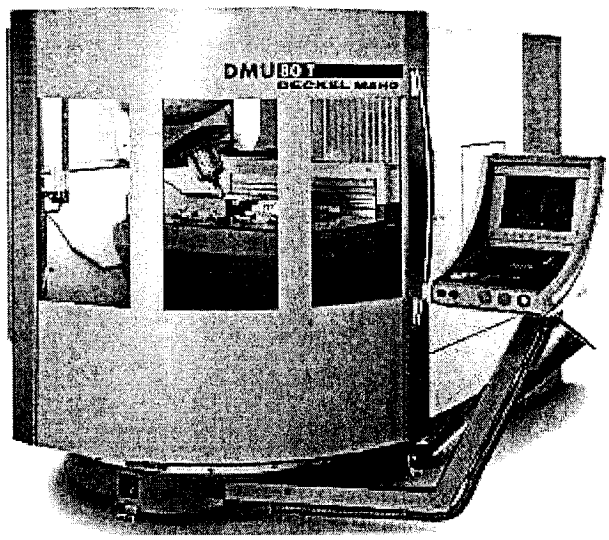

Figure 6.18 DECKEL MAHO CNC Milling Machine

The spindle speed is given by the following equation:

$$N = \frac{12 \cdot cs}{\pi \cdot D} \tag{6.1}$$

where N is spindle speed (*rpm*), D cutter diameter (*inch*), cs is cutting speed (*feet/min*). The cutting speed can be found in a machining handbook based on the workpiece and cutter material and the cutter size. For this particular machining test, the spindle speed is calculated at 5000 *rpm*.

Figure 6.19 Machined Part

In this machining, there are six layers to machine using difference feed rate sets. The first and second layers are machined with two constant feed rates (7 and 15 *inch/min*) for each tool path segment. These segments are defined in Figure 6.4. Layer (3) is set with a constant feed rate (*33 inch/min*) obtained in a machining handbook for all tool path segments. Layer (4) is set with a proper feed rate for all tool path segments based on the geometry features. In layer (5) a constant feed rate (45 *inch/min*) is set. In layer (6) the feed rate is set for all segments based on their geometry features. Table 6.2 shows those machining results.

From Table 6.2, it can be seen that feed rate is a very important factor for machining efficiency and surface quality. While a faster feed rate improves machining efficiency, an excessive feed rate causes chatter which harms surface quality. The proper feed rate is used in the layer (4) machining. It can easily be seen that the machining on the layer (4) has higher machining efficiency with good surface quality. The proper feed rate, based on the geometry features of the machined part, can ensure high machining efficiency with good surface quality.

Table 6.2 Machining Time and Surface Quality for Different Feed Rates

		Tool Path Segments						Machining Time	Surface Quality
		A-B	C-D	I-J	M-N	O-P	R-Q		
Feed Rate (*Inch/min*)	Layer(1)	7	7	7	7	7	7	3 min and 40 sec	No chatter
	Layer(2)	15	15	15	15	15	15	1 min and 45 sec	No chatter
	Layer(3)	33	33	33	33	33	33	47 sec	No chatter
	Layer(4)	40	39	37	35	44	33	39 sec	No chatter
	Layer(5)	45	45	45	45	45	45	34 sec	Chatter
	Layer(6)	54	52	50	47	60	45	29 sec	Chatter

Chapter 7 Summary and Contributions

7.1 Summary

This work proposes a generic and intelligent approach of feed rate determination for CNC profile machining. This approach is aimed at determining proper feed rates according to the geometries of the part profile for its CNC machining. The determined feed rates can ensure the high machining efficiency and prevent chatter in machining. It lays a foundation for the research on feed rate determination for multi-axis CNC machining. It can also be applied on feed rate determination on high speed machining.

It is a generic approach because a machining parameter database can be built for any type of tool and part material. It is an intelligent approach because a method to generate a multiple-input-and-single-output (MISO) fuzzy inference system based on any machining parameters database is introduced. The cutting force can be predicted once the radial and axial depth of cut and feed rate are input in the fuzzy inference system. It is important to be able to predict the maximum cutting force because it is closely tied to the search for the proper feed rate. The work introduces a generic method to handle practical problems, such as predicting the cutting force for different types of workpiece and tool material. By identifying the geometric features of the part profile, the proper

feed rate can be determined for each geometric feature and the CNC profile milling can be carried out with the different feed rates.

7.2 Contributions

The main contributions of this work can be summarized as follows:

- The approach proposed by Bae, *et al.*, (2003) [4] did not take the axial depth of cut into account, and it is impractical in CNC machining. This work solves this problem.
- Bae's method could not ensure the correct relationship between the cutting force and feed rate by using a Bezier surface. This work solves the problem by using a fuzzy logical system.
- The approach provided in this work optimizes feed rates based on the geometric features of a part, using a fuzzy rule-based system. Therefore, the feed rate for each geometry point can be precisely identified, based on the individual point's geometrical feature.
- The required surface quality and higher machining efficiency are the main objective of feed rate determination for part finishing. In this approach, the proper feed rate determination forms a kind of frame that controls a part machining in higher machining efficiency, and the fuzzy logical cutting force model fills the frame to ensure adequate surface quality.
- In general, the tool path traces the curve followed by the cutter, which passes through a number of cutter contact (CC) points as part of a continuous machining process. Using the approach presented in this work, the feed rate at each CC

point can be identified with great precision. The valuable result is an enrichment of the definition of the tool path.

7.3 Future Work

One problem that remains to be solved is developing the feed rate determination system with an automatic NC codes optimization function, which could directly generate the optimized NC codes. Another problem involves 5-axis CNC machining. In this work, the two-dimension chip load model is used to determine the proper feed rate for CNC profile milling with a 3-axis machine. Logically, the next problem to be solved is how to find a three-dimension chip load model that could determine the proper feed rate for 5-axis machining.

Publication

Chen, Z.C., and Miao, Z.B., "A Generic and Intelligent Approach of Feed Rate Determination for CNC Profile Milling," *Proceedings of the International Conference on Flexible Automation and Intelligent Manufacturing*, July 12-14, 2004, Toronto, Canada.

Chen, Z.C., and Miao, Z.B., "A Generic and Intelligent Approach of Feed Rate Determination for CNC Profile Milling;" to have been Submitted, International Journal of Computer Applications in Technology (IJCAT).

Bibliography

1. Altintas, Y., *Manufacturing Automation*, Cambridge University Press, 2000.

2. Alwedyan, H., Demirli, K., and Bhat, R., "A Technique for Fuzzy Logic Modeling of Machining Process," *Annual Conference of the North American Fuzzy Information processing Society - NAFIPS*, 2001, Vol. 5, pp. 3021-3026.

3. Asai, A., and Tsuruhashi, T., "Development of Die-Cutting Feed Rate Control System," *Japanese Associate of Engineering Review*, 1988, Vol. 9: pp. 72 - 82.

4. Bae, S.H., Ko, K., Kim, B.H., and Choi, B.K., "Automatic Feedrate Adjustment for Pocket Machining," *Computer-Aided Design*, 2003, Vol. 35, pp. 495 - 500.

5. Baek, D.K., Ko, T.J., and Kim, H.S., "Optimization of Feed Rate in a Face Milling Operation Using a Surface Roughness Model," *International Journal of Machine Tools & Manufacture*, 2001, Vol. 41, pp. 451 – 462.

6. Bailey, T., Elbestawi, M.A., Ei-Wardany, T.I., and Fitzpatrick, P., "Generic Simulation Approach for Multi-Axis Machining, Part 2: Model Calibration and Feed Rate Scheduling," *Journal of Manufacturing Science and Engineering*, August 2002, Vol. 124, pp. 634 – 642.

7. Chen, Z.C., *Ph. D. Dissertation Optimal and Intelligent Multi-Axis CNC tool Path Generation for Sculptured Part Machining*, Department of Mechanical Engineering University of Victoria, 2002.

8. Chen, Z.C., Dong, Z., and Vickers, G.W., "Optimal 3½½-Axis CNC Machining of Sculptured Parts Using Fuzzy Pattern Clustering," *Proceedings of the International*

ICSC Congress on Soft Computing and Intelligent Systems for Industry Symposium on Intelligent Systems for Industry, June 26 – 29, 2001, Scotland, UK.

9. Chen, Z.C., and Miao, Z.B., "A Generic and Intelligent Approach of Feed Rate Determination for CNC Profile Milling," *Proceedings of the International Conference on Flexible Automation and Intelligent Manufacturing*, July 12-14, 2004, Toronto, Canada.

10. Choi, B.K., and Jerard, R., *Sculptured Surface Machining – Theory and Applications*, Kluwer Academic Publishers, 1998.

11. Choi, B.K., and Park, S.C., "A Pair-Wise Offset Algorithm for 2D Point-Sequence Curve," *Computer-Aided Design*, 1999, Vol. 31, pp. 735 – 745.

12. Chui, S.L., "Fuzzy Model Identification Based on Cluster Estimation," *Journal of Intelligent and Fuzzy Systems*, 1994, Vol. 2, pp. 276 - 278.

13. Dermirli, K., *Lecture Notes of ENCS 6191 in Concordia University*, Fall, 2002.

14. *Fuzzy Logic Toolbox User's Guide*, The Mathworks, Inc, 1998.

15. Gibbs, D., and Crandell, T., *An Introduction to CNC Machining and Programming*, Industrial Press Inc., 1991.

16. Hansen, A., and Arbab, F., "An Algorithm for Generating NC Tool Paths for Arbitrarily Shaped Pockets with Islands," *Association for Computing Machinery Transactions on Graphics*, April 1992, Vol. 11, No. 2, pp. 152 -182.

17. Ip, W.L.R., "A Fuzzy Basis Material Removal Optimization Strategy for Sculptured Surface Machining Using Ball-nosed Cutters," *International Journal of Production Researches*, 1998, Vol. 36, No. 9, pp. 2553 – 2571.

18. Joseph, O, *Computational Geometry in C*, Cambridge University Press, 1998.

19. Kline, W.A., DeVor, D.A., and Lindberg, J.R., "The Prediction of Cutting Forces in End Milling with Application to Cornering Cuts," *International Journal of Machines and Tool Design Research*, 1982; 22(1) : pp. 7 - 22.

20. Ko, J.H., Cho, D.W., and Ko, T.J., "Off-Line Feed Rate Scheduling for 3D Ball-End Milling Using a Mechanistic Cutting Force Model," *Transaction of the North American Manufacturing Research Institution of Society of Manufacturing Engineers (NAMRI/SME)*, 2003, Vol. XXXI, pp. 113 – 120.

21. Ko, J.H., Yun, W.S., and Cho, D.W., "Off-Line Feed Rate Scheduling Using Virtual CNC Based on an Evaluation of Cutting Performance," *Computer-Aided Design*, 2003, Vol. 35, pp. 383 - 393.

22. Le Grand, R., Colvin, F.H. and Stanley, F.A., *The New American Machinist's Handbook*, McGraw-Hill Book Company, 1955.

23. Lee, J.M., Chu, C.N., Kim, S.Y., and Kim, B.H., "Feed-Rate Optimization of Ball End Milling Considering Local Shape Features," *Annals of the CIRP*, 1997, Vol. 46.

24. Liu, X.W., Cheng, K., Webb, D., and Luo, X.C., "Prediction of cutting force distribution and its influence on dimensional accuracy in peripheral milling," *International Journal of Machine Tools & Manufacture*, 2002, Vol. 42, pp. 791 - 800.

25. *Machining Data Handbook*, Metcut Research Associates Inc., 1980.

26. Madison, J., *CNC Machining Hand Book – Basic Theory Production Data and Machining Procedures*, Industrial Press Inc., 1996.

27. Meyers, A.R., and Slattery, T.J., *Basic Machining Reference Handbook*, Industrial Press Inc., 2001.

28. Moler, C., and Costa, P., *Symbolic Math Toolbox User's Guide*, The Math Works Inc, 1993.

29. Subrahmanyam, S., and Wozny, M., "An Overview of Automatic Feature Recognition Techniques for Computer Aided Process Planning," *Computers in Industry*, 1995, Vol. 26, pp. 1-21.

30. *Use of Computers in Numerical Control Programming*, Thomson Corporation, 2001.

31. Wang, L.X., *A Course in Fuzzy Systems and Control*, Prentice Hall PTR, 1997.

32. Yun, W.S., and Cho, D.W., "Accurate 3-D Cutting Force Prediction Using Cutting Condition Independent Coefficients in End Milling," *International Journal of Machine Tools & Manufacture*, 2001, Vol. 41, pp. 463 – 478.